

**Final Technical Report to the  
Department of Energy, National Energy Technology Lab  
Interagency Agreement DE-AT26-97FT34342  
September 1, 1997 – April 30, 2005**

**Task No. 6  
Preparation, Drilling, and Testing of a Gas Hydrate Well**

**INTEGRATED GEOLOGIC AND GEOPHYSICAL  
ASSESSMENT OF THE EILEEN GAS HYDRATE  
ACCUMULATION, NORTH SLOPE, ALASKA**

**By**

**Timothy S. Collett, David J. Taylor,  
Warren F. Agena, Myung W. Lee,  
John J. Miller & Margarita Zyrianova  
United States Geological Survey  
Denver Federal Center  
MS-939, Box 25046  
Denver, Colorado 80225  
Email: [tcollett@usgs.gov](mailto:tcollett@usgs.gov)  
Phone: 303.236.5731**

**Tanya L. Inks  
IS Interpretation Services, Inc.**

**April 1, 2005**

*Disclaimer: This report was prepared as an account of work sponsored by an agency of the United States Government. Neither the United States Government nor any agency thereof, nor any of their employees, makes any warranty, express or implied, or assumes any legal liability or responsibility for the accuracy, completeness, or usefulness of any information, apparatus, product, or process disclosed, or represents that its use would not infringe privately owned rights. Reference herein to any specific commercial product, process, or service by trade name, trademark, manufacturer, or otherwise does not necessarily constitute or imply its endorsement, recommendation, or favoring by the United States Government or any agency thereof. The views and opinions of authors expressed herein do not necessarily state or reflect those of the United States Government or any agency thereof.*

## ABSTRACT

Using detailed analysis and interpretation of 2-D and 3-D seismic data, along with modeling and correlation of specially processed log data, a viable methodology has been developed for identifying sub-permafrost gas hydrate prospects within the Gas Hydrate Stability Zone (HSZ) and associated “sub-hydrate” free gas prospects in the Milne Point area of northern Alaska (**Figure 1**). The seismic data, in conjunction with modeling results from a related study, was used to characterize the conditions under which gas hydrate prospects can be delineated using conventional seismic data, and to analyze reservoir fluid properties. Monte Carlo style gas hydrate volumetric estimates using Crystal Ball™ software to estimate expected in-place reserves shows that the identified prospects have considerable potential as gas resources. Future exploratory drilling in the Milne Point area should provide answers about the producibility of these shallow gas hydrates.

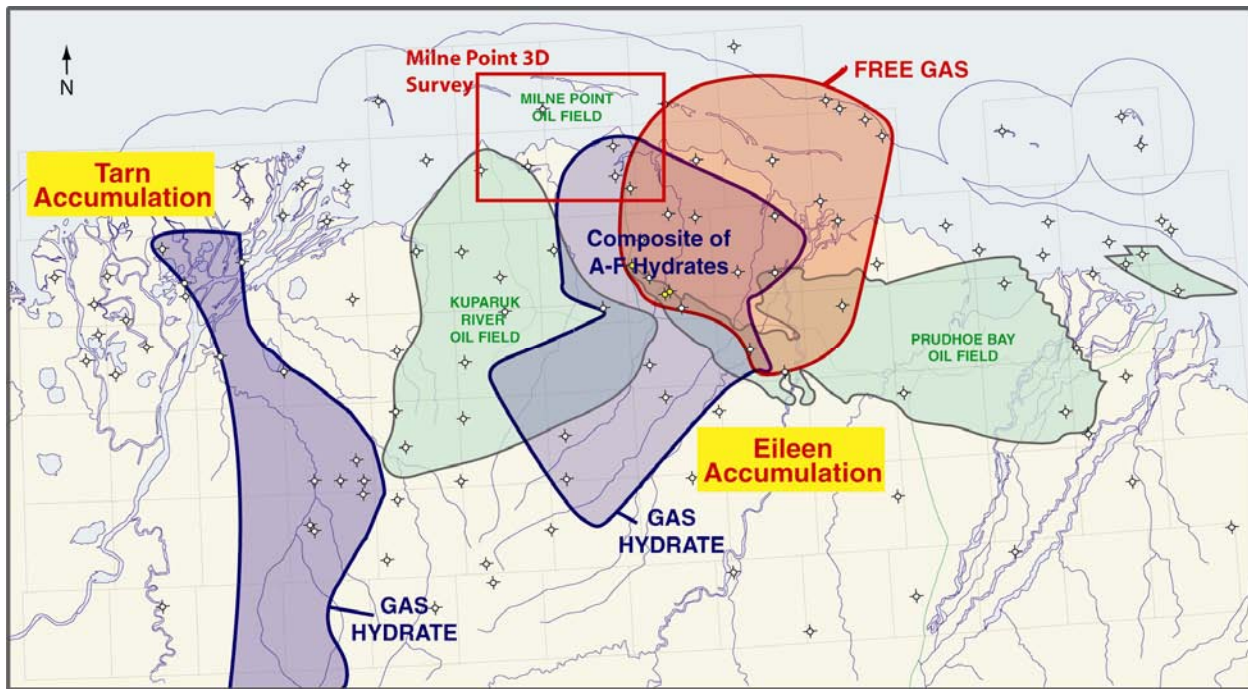


**Figure 1.** This map shows the Milne Point 3-D study area and identified gas hydrate accumulations. The Milne Point study area is in the northern-most part of the “Eileen Accumulation”. The study area is adjacent to the prolific Kuparuk River and Prudhoe Bay oil fields.

## **TABLE OF CONTENTS**

<b>INTRODUCTION</b>	<b>7</b>
<b>EXECUTIVE SUMMARY</b>	<b>9</b>
<b>GEOLOGICAL SETTING</b>	<b>10</b>
Base of IBPF to BHSZ -- “Zone of Interest”	13
<b>SYNTHETIC LOG CORRELATION</b>	<b>15</b>
<b>SEISMIC DATA PREPARATION</b>	<b>17</b>
Trace Modeling	17
Petrophysical Analysis	21
Reflection Coefficient versus Gas Hydrate Saturation	24
Seismic Stratigraphic Correlation	25
<b>PROSPECTING</b>	<b>27</b>
Intra Gas Hydrate Prospects	34
<b>GAS HYDRATE VOLUMETRIC ESTIMATES</b>	<b>43</b>
<b>CONCLUSIONS</b>	<b>46</b>
<b>REFERENCES</b>	<b>47</b>

## **LIST OF GRAPHICAL MATERIALS**

**Figure 1.** This map shows the Milne Point 3-D study area and identified gas hydrate accumulations. The Milne Point study area is in the northern-most part of the “Eileen Accumulation”. The study area is adjacent to the prolific Kuparuk River and Prudhoe Bay oil fields.

**Figure 2.** This graph is a phase diagram for the Hydrate Stability Zone in on-shore Arctic regions. Hydrates co-exist with permafrost in the interval between about 200 and 600 m. ( $\approx$  650-1970 ft) at Milne Point.

**Figure 3.** Map shows Milne Point area faulting at approximately the Top of the Staines Tongue of the Sagavanirktok Formation. The Top Staines Tongue is near the Base of the Hydrate Stability Zone over much of the survey. The gas hydrate study was limited to the on-shore portion of the seismic survey.

**Figure 4.** Stratigraphic columns used in the Milne Point study showing regional stratigraphic markers and their relationship to Gas Hydrate “C” picks developed by Collett (1993).

**Figure 5.** Gamma ray and resistivity logs from the Kuparuk River area showing the Eileen gas hydrate accumulation (Units A-F) (modified from Collett, 1993).

**Figure 6.** This map shows the BHSZ time structure map for the Milne Point study area generated using well derived temperature data and IBPF picks from well logs data.

**Figure 7.** This synthetic seismogram to seismic tie panel for the CO MPU B-2 well shows the excellent tie between the synthetic seismogram and correlative piece of 3-D seismic at the well. Minimal stretch was required for the tie.

**Figure 8.** USGS reprocessing improved the power spectrum of the 3D seismic data, increasing the over-all frequency within the zone of interest and whitening the spectrum. This display is a comparison, within the shallow Hydrate Stability Zone, before and after wavelet reprocessing.

**Figure 9.** The display shows an example line before and after USGS wavelet reprocessing. The yellow outlined area shows where the USGS signature wavelet deconvolution sharpens the wavelet and broadens the frequency spectrum. The red outlined area show where the USGS predictive deconvolution suppressed interbed multiple reflections.

**Figure 10.** This model shows the seismic response to increasing hydrate thickness. Gas Hydrates greater than about 20 ft thick show an obvious amplitude increase at the Top C Hydrate and Base C Hydrate with all other events remaining constant.

**Figure 11.** This model shows the trace response to a dipping model, at normal SEG polarity. The thin-bed response shows a phase change and amplitude change that is very similar to the actual seismic events near the Base Hydrate Stability Zone (BHSZ). The thick hydrate shows a pull-up and the gas a push-down on the flat model base related to velocity within the reservoir interval.

**Figure 12.** The log suite MPU S-15 well is shown with calculated petrophysical curves for water saturation ( $S_w$ ) and water resistivity ( $R_w$ ) at various salinities. Coals are found only in the interval below the Top Staines Tongue of the Sagavanirktoq in this and other Milne Point wells.

**Figure 13.** The log suite of the Cascade #1 well is shown with calculated petrophysical curves for water saturation ( $S_w$ ) and water resistivity ( $R_w$ ) at various salinities.

**Figure 14.** This seismic display is a line from a reflection strength volume. Parallel green and yellow lines depict the margin of error in the calculated Base Hydrate Stability Zone (BHSZ, from log data).

**Figure 15.** This seismic line is a color variable density display from the amplitude volume. The zone of interest is between the C16 Seismic marker (dark green) and the parallel green and yellow lines which represent the margin of error for the Base Gas Hydrate Stability Zone (BHSZ) horizon. The abrupt terminations of amplitude near the minimum base of the Hydrate Stability Zone (Min BHSZ) are interpreted as gas trapped by the hydrate.

**Figure 16.** The Eileen gas hydrate correlations from Collett (1993). The “B” through “E” Gas Hydrate Units are within the Hydrate Stability Zone at Milne Point. “E” and “D” gas hydrate units are commingled with permafrost in some parts of Milne Point.

**Figure 17.** The Intra-Hydrate prospect reconnaissance map within the Gas Hydrate Stability Zone shows the Maximum absolute amplitude from 50 ms below the C16 Seismic Marker to 50 ms. above the Upper Staines Tongue Marker. Several areas of interest were identified, including the Mt. Elbert “C” hydrate anomaly.

**Figure 18.** The minimum and maximum Base Hydrate Stability Zone events are shown relative to truncated high amplitude seismic reflections that are interpreted to be sub-hydrate free gas accumulations.

**Figure 19.** This seismic line shows the thick, nearly reflectionless, Canning Shale zone separating the Hydrate Stability Zone interval from the deeper Ellesmarian section that produces oil and gas in Milne Point, Kuparuk River and Prudhoe Bay fields. Some larger regional faults can be seen cutting this interval.

**Figure 20.** This display shows a shallow coherency timeslice with various fault trends. Older faults, trending more NE to SW, are more likely to be conduits for hydrocarbon migration.

**Figure 21.** This display shows Milne Point gas hydrate prospects developed by 3D seismic analysis.

**Figure 22.** The CO MPU B-2 well tie, down-dip of Mt. Elbert C and D hydrate anomalies show thin hydrates identified on logs. These hydrates are below the detection limits of the seismic (less than 25 ft thick.) Amplitude anomalies in the up-thrown block correlate to these hydrates and are interpreted to be thicker, high saturation hydrates.

**Figure 23.** This 3-D display of the fault bounded Mt. Elbert prospect amplitude horizon shows the relationship of the anomaly to bounding faults and wells.

**Figure 24.** The Maroon Peak free gas and gas hydrate prospects are shown by amplitude and phase variations. The “Free Gas” anomalies are represented by a peak, and the “Hydrate” in the up-thrown block is represented by a trough on this reverse SEG polarity data.

**Figure 25.** This display shows the Mt. Elbert “C” Hydrate events used in Lee’s saturation calculation. The Seismic line shows the tie across the fault to the BP MPU E-26 well.

**Figure 26.** This display is a thickness map for the Mt. Elbert prospect. Thicknesses were derived using Lee’s thin-bed analysis.

**Figure 27.** This display is a saturation map for the Mt. Elbert prospect. Saturations were derived using Lee’s thin-bed analysis.

## INTRODUCTION

In on-shore Arctic regions, the Gas Hydrate Stability Zone (HSZ) typically occurs at the depths and temperatures defined by the methane hydrate phase diagram shown in **Figure 2**. In September 2003, a DOE funded study was initiated by the United States Geological Survey (USGS) to assess existing data from the Milne Point area of Northern Alaska in order to characterize the resource potential of the HSZ in the interval between the base of ice bearing permafrost (IBPF) at a depth of around 600 meters and the base of the Hydrate Stability Zone (BHSZ) at around 1100 meters in the Milne Point area on the North Slope of Alaska. A 3-D seismic data set provided to the USGS by BP Exploration Alaska, Inc. (**Figure 3**, red outline) was used as the foundation for this *seismic driven* study. A variety of other data including a small portion of the NW Eileen 3-D survey just to the south of the Milne Point survey (**Figure 3**, blue outline), USGS owned regional 2-D seismic data (**Figure 3**, white lines), well log data and cultural information. The historical work of Collett (1993,1992) was used to constrain and improve the quality of critical maps, such as time structure maps, fault maps and base Hydrate Stability Zone maps, in the Milne Point area. Shown in **Figure 3** is a map of the Milne Point area depicting the location of the 2-D and 3-D seismic data used in this study.

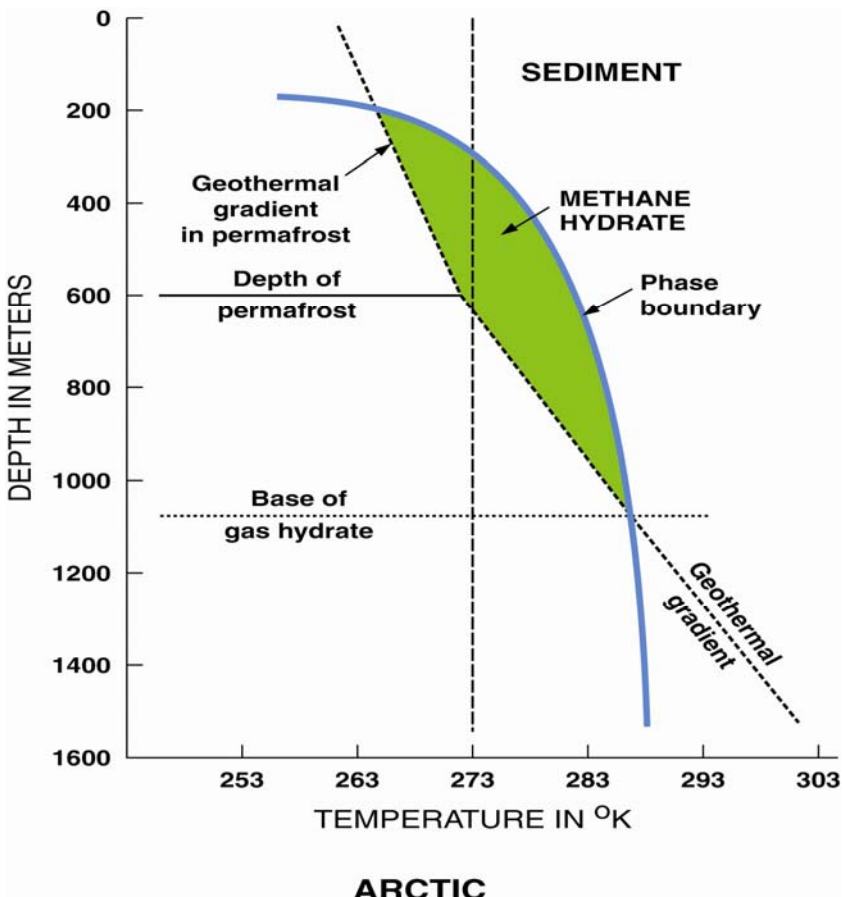


**Figure 2.** This graph is a phase diagram for the Hydrate Stability Zone in on-shore Arctic regions. Hydrates co-exist with permafrost in the interval between about 200 and 600 m. ( $\approx 650\text{-}1970$  ft) at Milne Point.

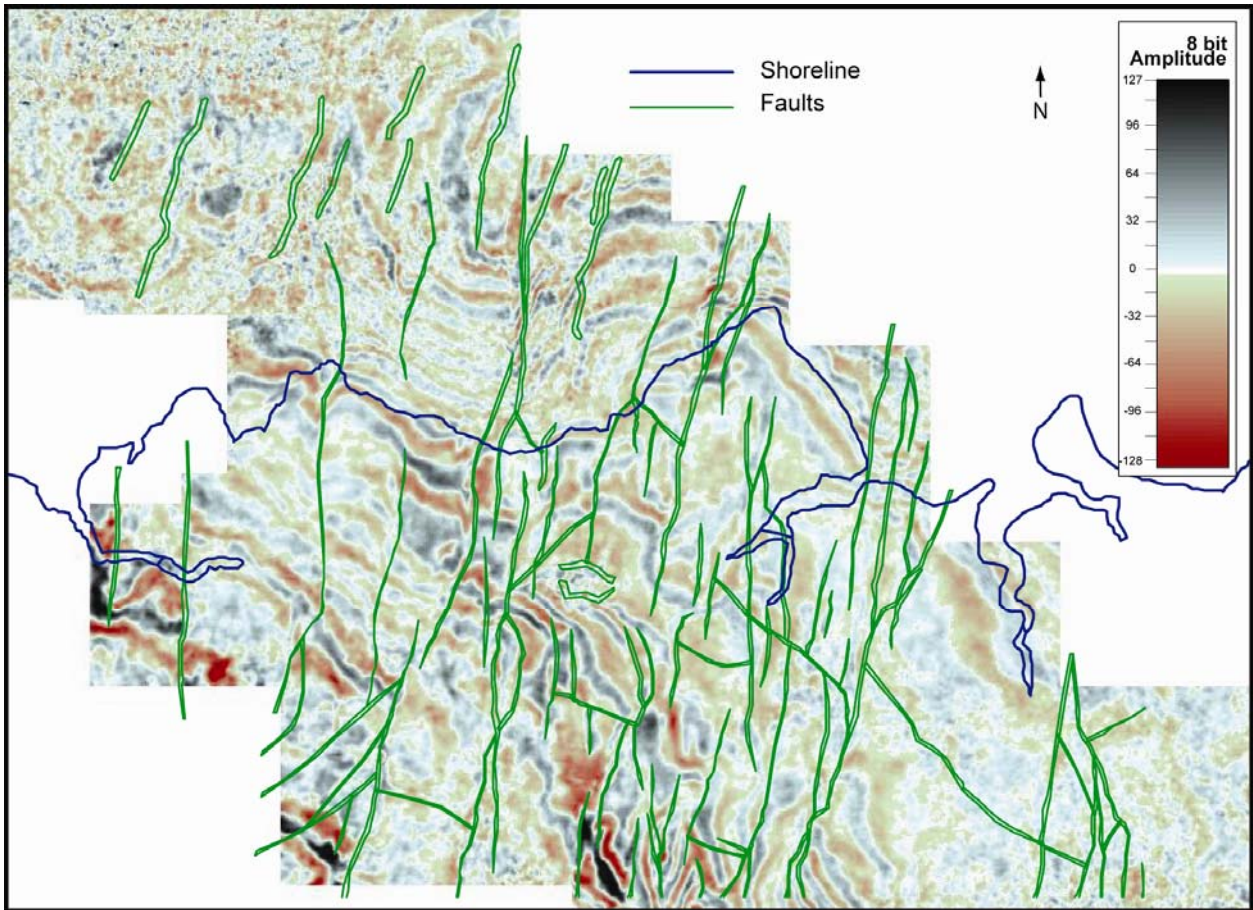


**Figure 3.** Map shows Milne Point area faulting at approximately the Top of the Staines Tongue of the Sagavanirktok Formation. The Top Staines Tongue is near the Base of the Hydrate Stability Zone over much of the survey. The gas hydrate study was limited to the on-shore portion of the seismic survey.

## **EXECUTIVE SUMMARY**

In September 1997 a study was initiated, using 3-D seismic in the Milne Point area of northern Alaska, in support of a proposed drilling program that will help answer questions about gas-hydrate reservoir properties, possible production methods, and economics. Historical log correlation work and analysis of gas hydrates in the Milne Point area was used as a starting point for the analysis of the Milne Point 3-D seismic data block. Modern 3-D and 2-D seismic data was used to gain a better understanding of the geologic controls related to gas hydrate petroleum systems in the Milne Point area. The Landmark software suite was used to integrate and analyze detailed log correlations, specially processed log data, gas-hydrate composition information and specialized 3-D seismic volumes. Structural and stratigraphic interpretation of the 3D data were performed in the interval that includes the Base of Ice Bearing Permafrost (IBPF), the Hydrate Stability Zone and the gas bearing immediately below the Base of the Hydrate Stability Zone (BHSZ).

The seismic data was also used to analyze reservoir fluid properties the stack domain in comparison to theoretical seismic modeling results. The modeling showed that a relatively strong impedance contrast will occur when moderate to highly saturated gas hydrates exist within the Hydrate Stability Zone. Modeling shows that these shallow hydrates and the trapped sub-hydrate gas that is associated with them may cause velocity anomalies that would effect the depth conversion of deeper, conventional hydrocarbon targets in the North Slope region. The primary result of the study has been the development of viable “intra-hydrate” stability zone prospects and “sub-hydrate” free gas prospects. These prospects have been analyzed relative to the petrophysical parameters in analog wells, for comparable reservoir intervals. Monte Carlo style volumetrics were performed using Crystal Ball™ software to estimate expected in-place reserves. Future exploratory drilling in the Milne Point area will help answer questions about the potential of these shallow gas hydrates as a source for gas production.

## **GEOLOGICAL SETTING**

A mixture of microbial and thermogenic methane gases are known to comprise the gas hydrates found on the North Slope. The thermogenic gas has migrated episodically into and through the Cretaceous-Tertiary Canning Formation from sources in the Ellesmerian sequence. In our study area, the majority of the gas hydrates are found in the unconsolidated sandstone reservoirs of the Tertiary-Cretaceous Sagavanirkto Formation. The interpretation of the structural framework in the Milne Point 3-D seismic survey area shows that faulting may play a significant role in the migration and trapping of the gas associated with the gas-hydrate accumulations. **Figure 3** shows a representative interpreted fault pattern based on 3-D seismic in the Milne Point 3-D and NW Eileen 3-D surveys. The age relationship between various fault sets may play a significant role in determining migration pathways and the compartmentalization of these gas-hydrate prospects. Fault analyses on a 3-D seismic volume enhanced by coherency processing show that the fault orientation, above and below the Canning Formation, is distinctly different, and as such, the secondary and tertiary migration from Ellesmarian reservoirs are more complex than originally thought.

The Milne Point 3-D seismic interpretation utilized a stratigraphic column compiled from historical geologic picks from several sources. Conventional North American Chronostratigraphic nomenclature and North Slope regional correlations were combined (along with their corresponding age boundaries) from various sources. A complete set of formation names are shown in the “Chronostratigraphic” column in **Figure 4**, taken from the work of USGS researchers Bird and Magoon (1987). A Milne Point Stratigraphic Column, and C-Unit column (Collett, 1993) used in the Milne Point 3-D seismic interpretation project breaks down the Recent through Upper Cretaceous interval into another set of boundaries based on the Milne Point correlations and the gas hydrate work of Collett (1993). Individual gas hydrate units within the Milne Point study are labeled A through E according to the naming convention established by Collett (1993) for the regional Eileen gas hydrate study and are shown in **Figure 5**.

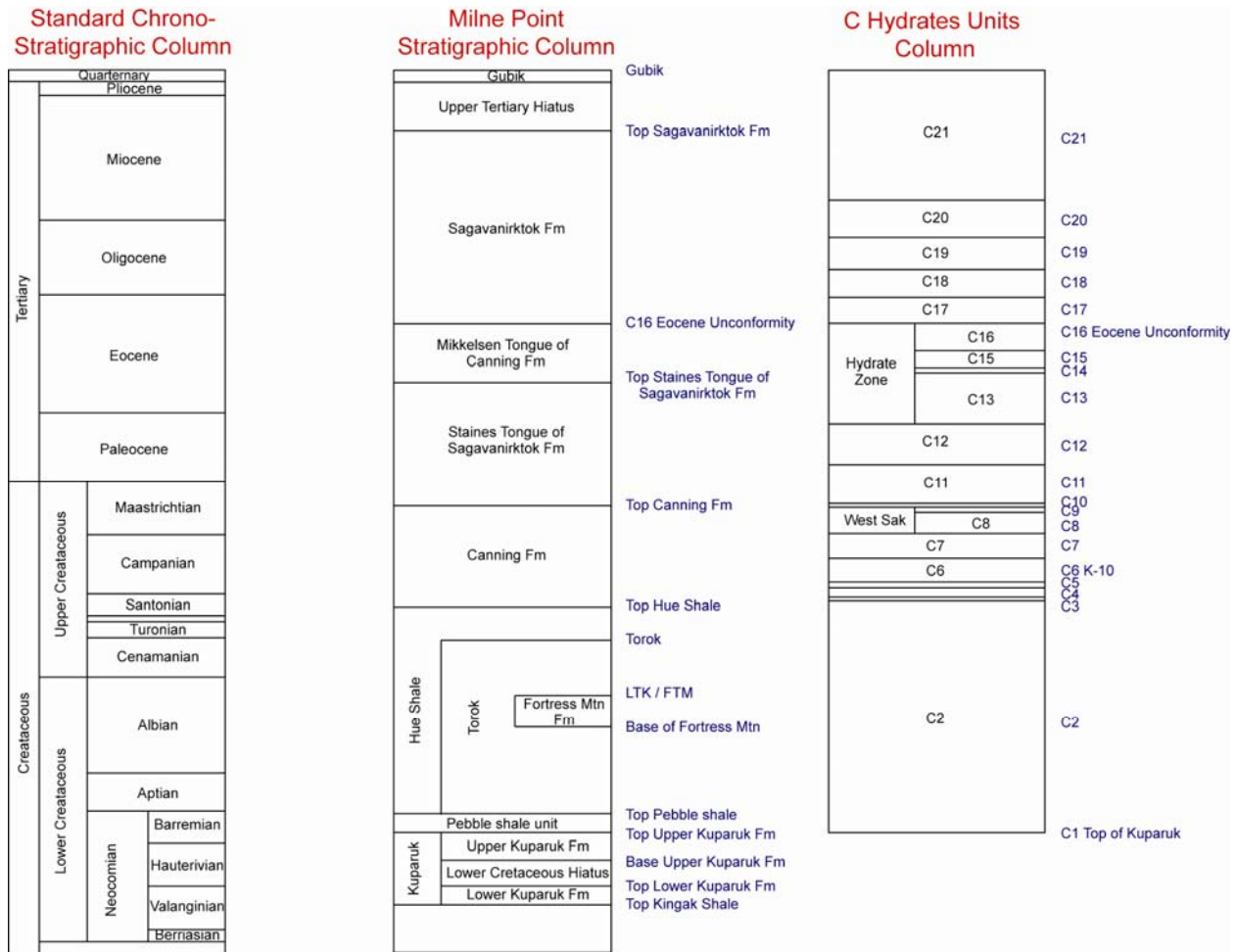


**Figure 4.** Stratigraphic columns used in the Milne Point study showing regional stratigraphic markers and their relationship to Gas Hydrate “C” picks developed by Collett (1993).

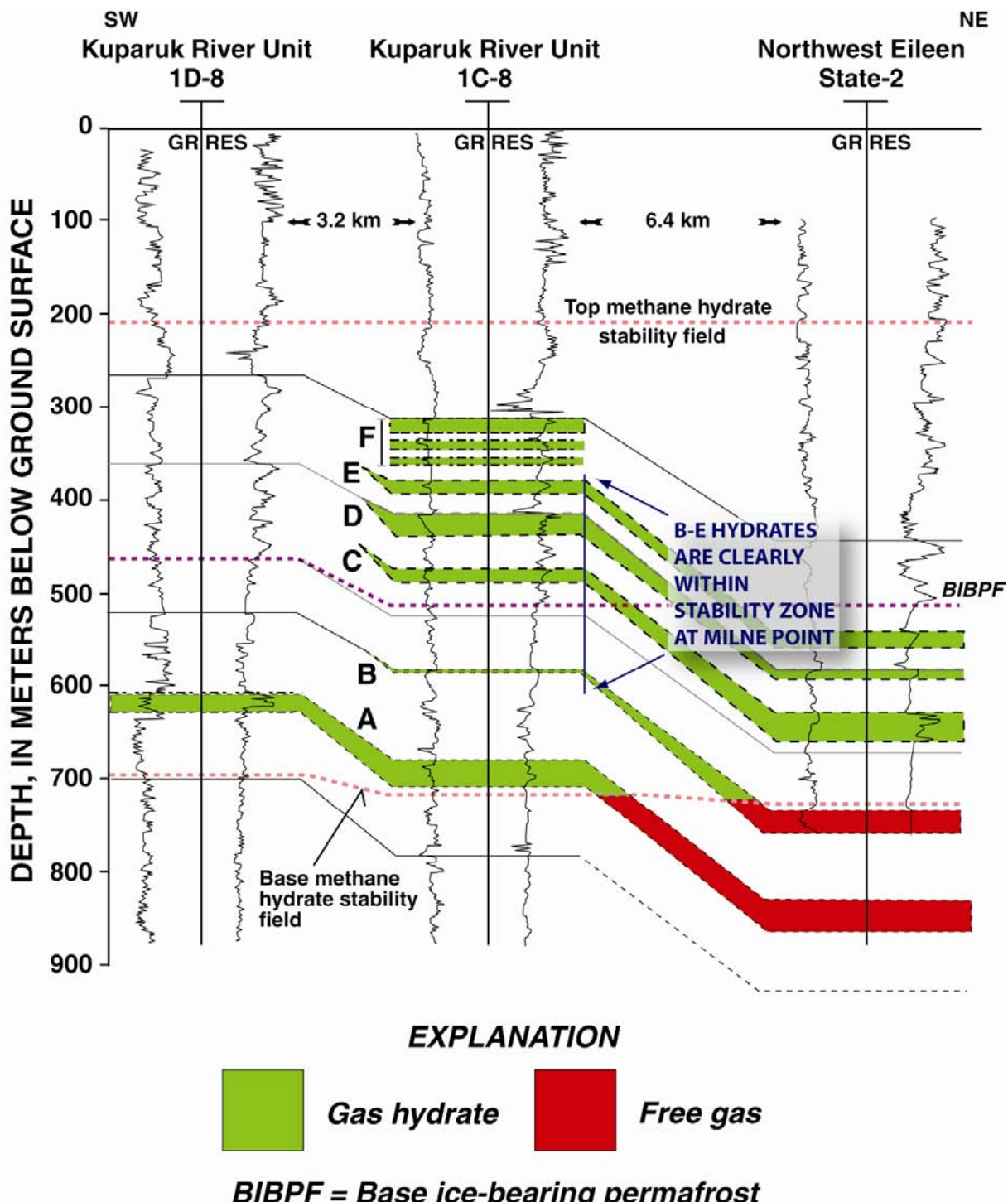


**Figure 5.** Gamma ray and resistivity logs from the Kuparuk River area showing the Eileen gas hydrate accumulation (Units A-F) (modified from Collett, 1993).

## **Base of IBPF to BHSZ -- “Zone of Interest”**

Digital well log data from several sources including USGS databases, industry, IHS, and the Alaska Oil and Gas Conservation Commission (AOGCC) was used to correlate geologic information within the “zone of interest” to seismic reflections and amplitude information within the 3-D seismic volume. Both the base of IBPF and the BHSZ was mapped within our area of interest. High resolution temperature logs were used to directly identify the base of the Hydrate Stability Zone (BHSZ). Depths to the BHSZ in the MPU A-1, MPU C-1, and MPU D-1 were identified at 2741, 2688, and 2836 feet respectively. For wells without high-resolution temperature logs, resistivity and velocity logs were used to make picks identifying the base of the ice bearing permafrost (IBPF). Once the base of IBPF was identified, a computer program developed at Colorado School of Mines (Sloan, 1997) was used to determine the BHSZ based on a predicted temperature gradient measured from the base of the IBPF (Table 1.) **Figure 6** shows the resulting time structure of the BHSZ using depths calculated from wells within or near the survey area.

Well	Ice-Bearing permafrost depth (MD, ft)	Temperature at the base of IBPF (deg F)	Depth to BHSZ (MD, ft)	Pressure at BHSZ (lbs/in <sup>2</sup> ) (from CSM)	Temp. at base of BHSZ (deg F) (from CSM)	Sub-IBPF geothermal gradient (deg F/100 ft)
MPU E-26	1760	30.2	2820	1221.1	53	2.15
Kaverak Pt 32-25	1796	30.2	2856	1236.6	54	2.25
MPU A-1	1708	30.2	2741	1186.9	53	2.21
MPU D-1	1783	30.2	2836	1228.0	53	2.17
West Sak 25	1821	30.2	2899	1255.3	54	2.21
MPU C-1	1678	30.2	2688	1163.9	53	2.26
MPU B-1	1808	30.2	2853	1235.3	54	2.28
MPU B-2	1806	30.2	2852	1234.9	54	2.28
MPU S15i	1910	30.2	3051	1321.1	55	2.17
MPU L-1	1858	30.2	2918	1263.5	54	2.25
West Sak 17	1738	30.2	2788	1207.2	53	2.17
Cascade	1674	30.2	2711	1173.9	53	2.2

AVG. Gradient	2.22
---------------	------

**Table 1.** Depths to base of IBPF and BHSZ in wells within the study area based on well logs only.

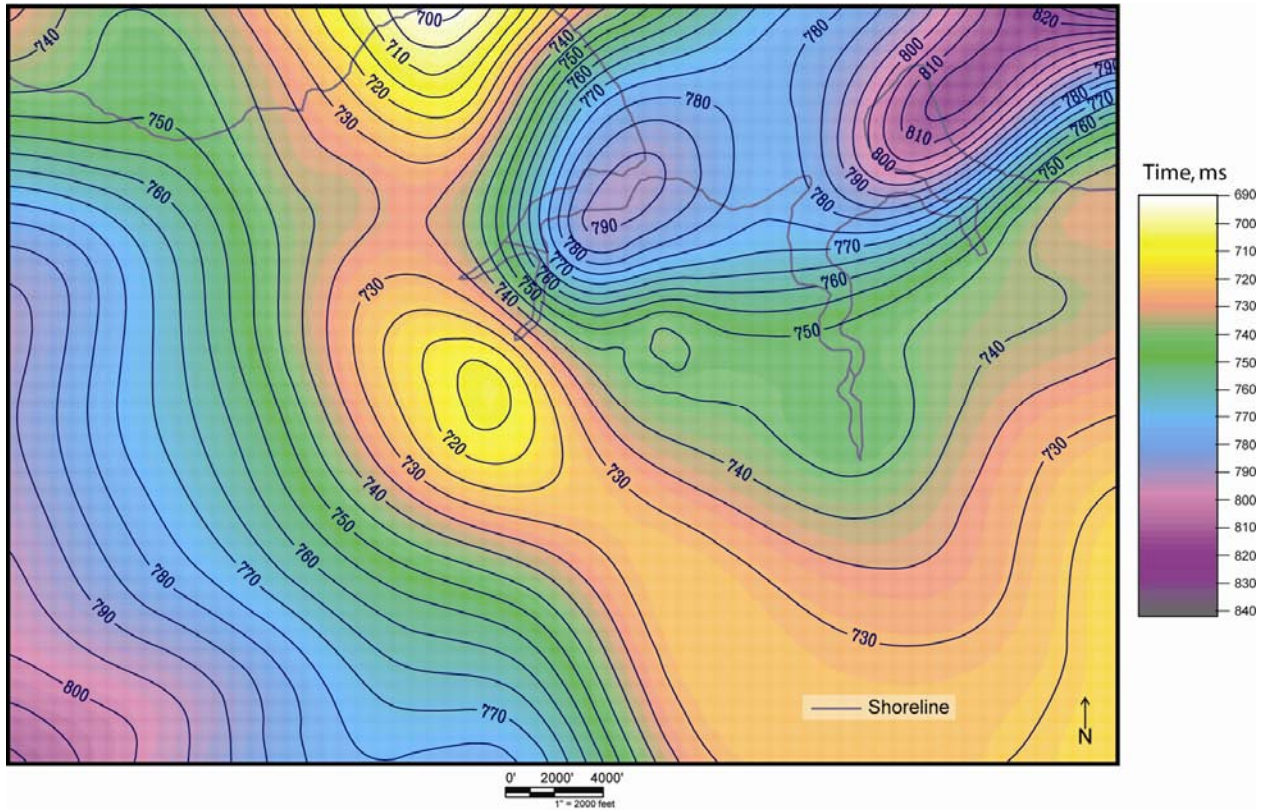


**Figure 6.** This map shows the BHSZ time structure map for the Milne Point study area generated using well derived temperature data and IBPF picks from well logs data.

## **SYNTHETIC LOG CORRELATION**

Preparation for the analysis of gas hydrates in the Milne Point project required definitive ties from geologic analysis of well log data to seismic character analysis. In order to accomplish this, careful synthetic to seismic correlations, petrophysical modeling, and trace modeling were required for meticulous integration of geological and geophysical data. In permafrost and unconsolidated sediments of the Saganavirktok Formation, logging problems are common. The most common problems are due to hole conditions, cycle skips in recording sonic log data, recording through casing points, and incomplete logging runs that do not extend to the surface. The shallow area of interest, typically in the upper 2000 ft., was therefore particularly affected by these problems. In many cases a substitute acoustic log was generated by modeling electrical resistivity well log data in the permafrost zone using a process developed by Lee (2006). Lee showed that P-wave velocity can be predicted from resistivity logs within permafrost or gas hydrate bearing sediments. Lee used resistivity logs to calculate gas-hydrate saturations and then was able to calculate P-wave velocity using these saturations as well as porosity, and estimated clay content. As a result, synthetic seismograms made by using a combination of derived and actual acoustic logs could be matched much more accurately to the seismic data. **Figure 7** shows the synthetic tie with the input log data, basic synthetic seismogram, and adjacent 3-D seismic data.

Our study utilized synthetic and pseudo-synthetic character ties for the time depth correlation. Synthetic ties for several wells were considered to be excellent, with the best (in the MPU B-2 well) having a correlation coefficient of greater than 70%. Checkshots were also reviewed for the Cascade, Kavearak and MPU L-1 wells and the MPU S-15 well VSP data. A 100 millisecond shift in the seismic data was applied to checkshots which confirmed our synthetic correlations. The 100 ms shift (which was applied to the seismic very early in the seismic processing) must be kept in mind for any depth conversion done at a later date, as it does affect the apparent velocity of the shallowest layer. Confirmation of these synthetic ties occurred when it could be shown that the tops correlation from well-to-well occurred along consistent seismic events. These correlations also confirmed that the historical markers correspond to time correlative surfaces.

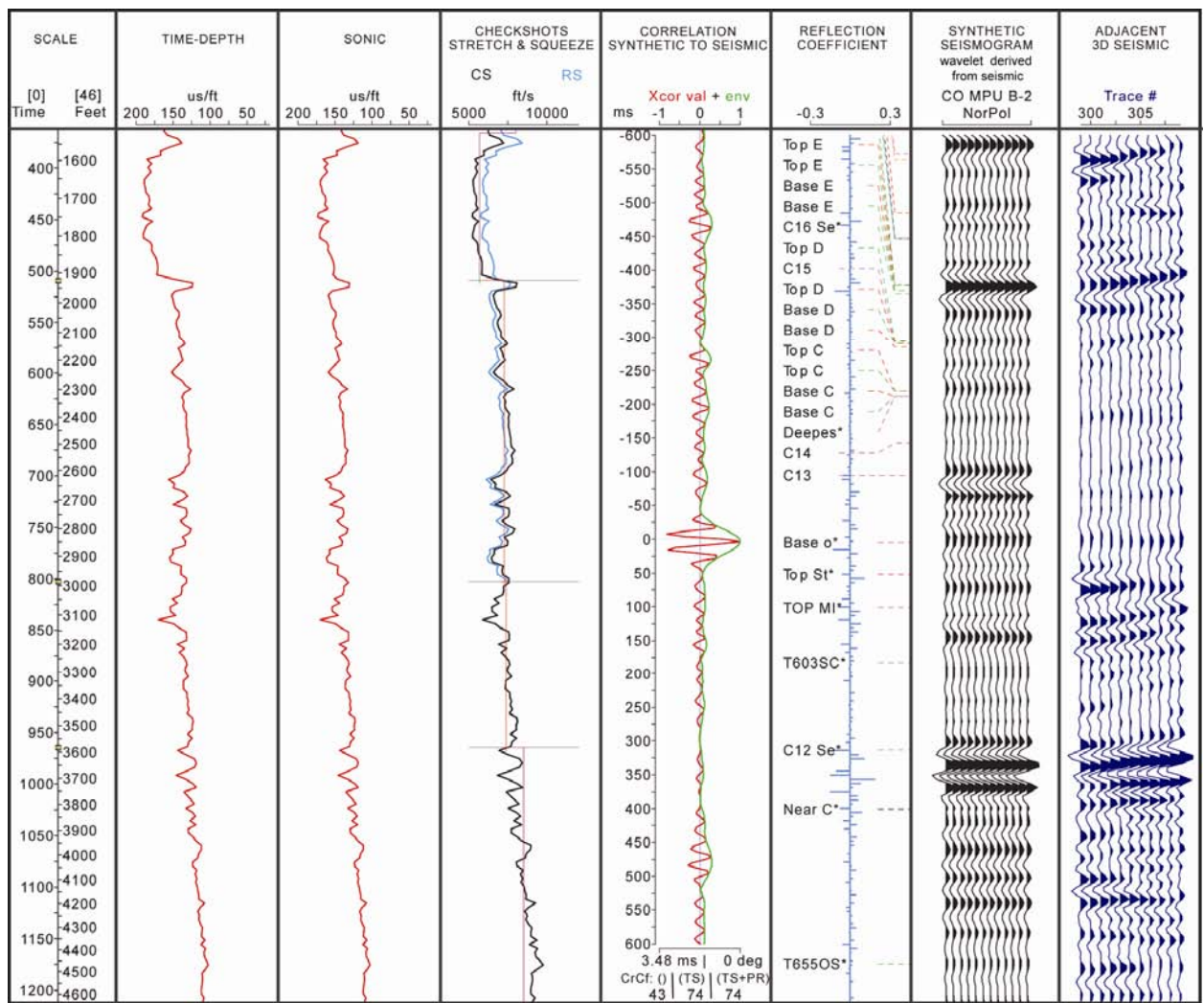


**Figure 7.** This synthetic seismogram to seismic tie panel for the CO MPU B-2 well shows the excellent tie between the synthetic seismogram and correlative piece of 3-D seismic at the well. Minimal stretch was required for the tie.

## **SEISMIC DATA PREPARATION**

Prior to interpretation, the USGS re-processed both the 2-D and 3-D seismic in order to maximize the interpretability of the data. As can be seen in the before and after images of **Figures 8 and 9**, the reprocessing, which included detailed velocity analysis, wavelet compression, interbed multiple suppression, and broadening of the frequency spectrum successfully improved the temporal resolution of the data.

### ***Trace Modeling***

Two trace models were used to understand the variations in seismic character between wells. Anomalous seismic amplitudes within the hydrate stability field appear to be thicker, highly saturated gas hydrate sections according to both wavelet and trace models. High amplitude events that abruptly dim at the BHSZ into the overlying section appear to be gas hydrate trapped gases. Additionally the models show that velocity effects may occur that pull up or push down deeper horizons under gas hydrates or gas bearing sections in this shallow part of the section.

#### **Case 1 – Intra-Hydrate reservoir with varying thicknesses**

The MPU B-2 well was used as a starting point to look at the effect of increasing thickness of gas hydrate reservoirs. The model well on the far left of **Figure 10** is the un-edited MPU B-2 well, with about 3.5 ft of gas hydrate. Because this gas hydrate is so thin, the acoustic response is suppressed, indicating lower saturations than can be actually detected.

The third well shows the same 3.5 ft thick gas hydrate with an acoustic response that would be appropriate for an 80% saturated gas. The fourth well shows a 10 ft thick gas hydrate section with 80% gas saturation. The fifth well shows a 20 ft thick gas hydrate with 80% gas saturation, and the last well on the right, shows a 40 ft thick gas hydrate with 80% gas saturation. The seismic response is predictable – amplitude increases with increasing thickness. Additionally, no significant response is seen until the thickness increases to about 20 feet.

#### **Case 2 – Dipping reservoir that crosses the BHSZ**

Shown in **Figure 11** is the model and synthetic seismic section for a dipping section that is used to model the response of the transition zone from gas hydrate, to gas, to water. The well on the left has a 10 ft. thick section of gas hydrate only. The second well on the left has a 20 ft. thick section of gas hydrate. The third well is a transitional well with a 10 ft. thick section of gas hydrate over a 10 ft. thick section of gas. The fourth well has a 20 ft. thick section of gas. And the well to the far right well has 20 ft. thick section of water saturated sand. In order to see the velocity effects from gas hydrate or gas, a horizontal bed was placed below the dipping horizon. Note the expected pull up under the gas hydrate reservoir at the modeled deeper horizon, which was entered as a flat, horizontal stratigraphic section. An acoustic push down can be seen in this event below the modeled gas reservoir as well.

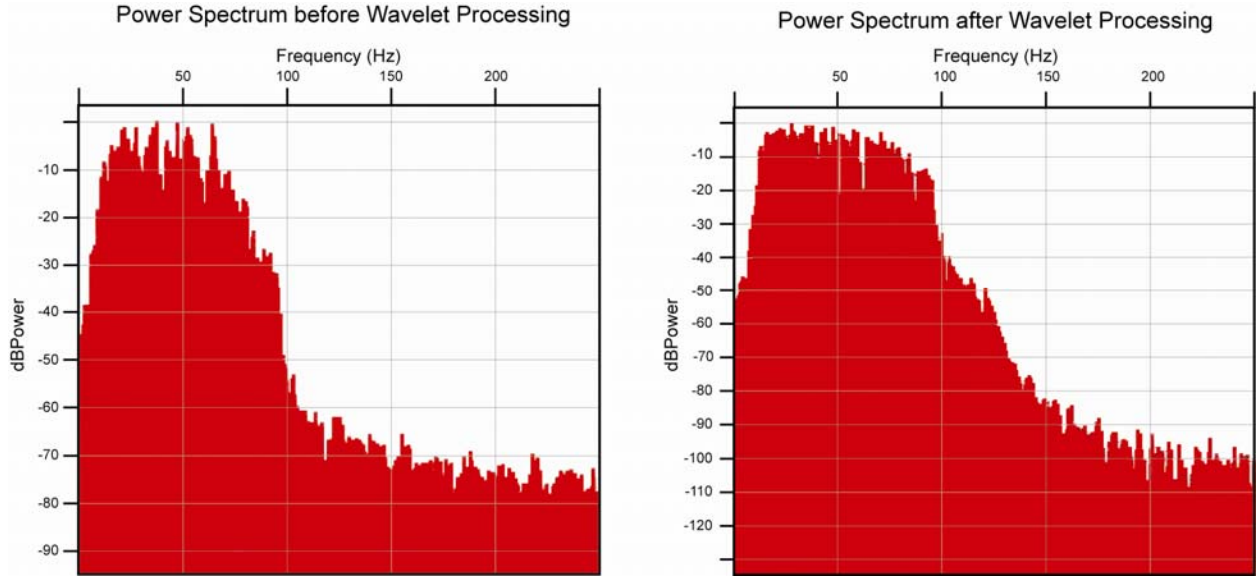


**Figure 8.** USGS reprocessing improved the power spectrum of the 3D seismic data, increasing the over-all frequency within the zone of interest and whitening the spectrum. This display is a comparison, within the shallow Hydrate Stability Zone, before and after wavelet reprocessing.

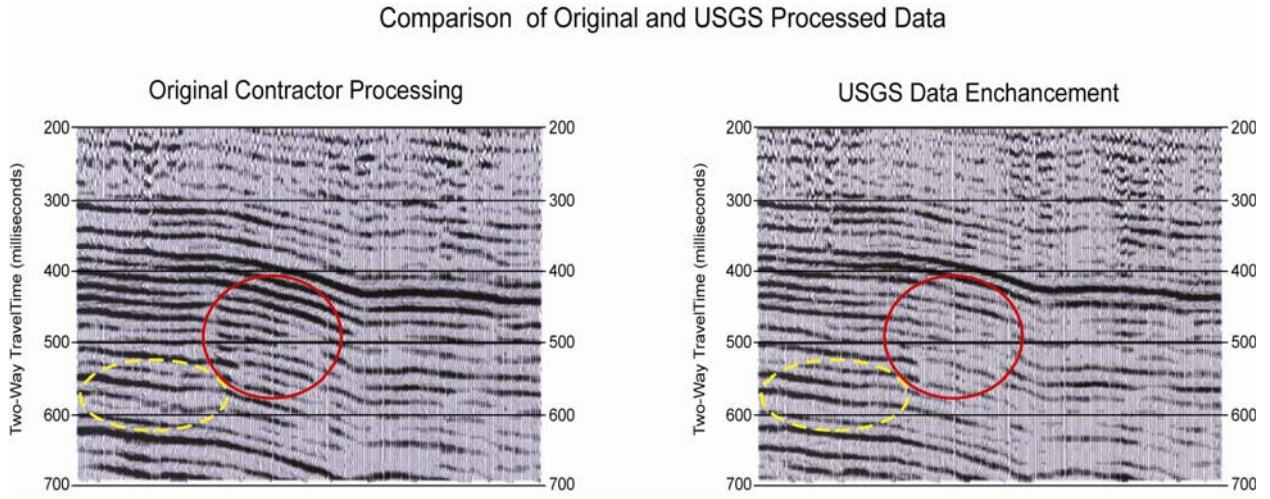


**Figure 9.** The display shows an example line before and after USGS wavelet reprocessing. The yellow outlined area shows where the USGS signature wavelet deconvolution sharpens the wavelet and broadens the frequency spectrum. The red outlined area shows where the USGS predictive deconvolution suppressed interbed multiple reflections.

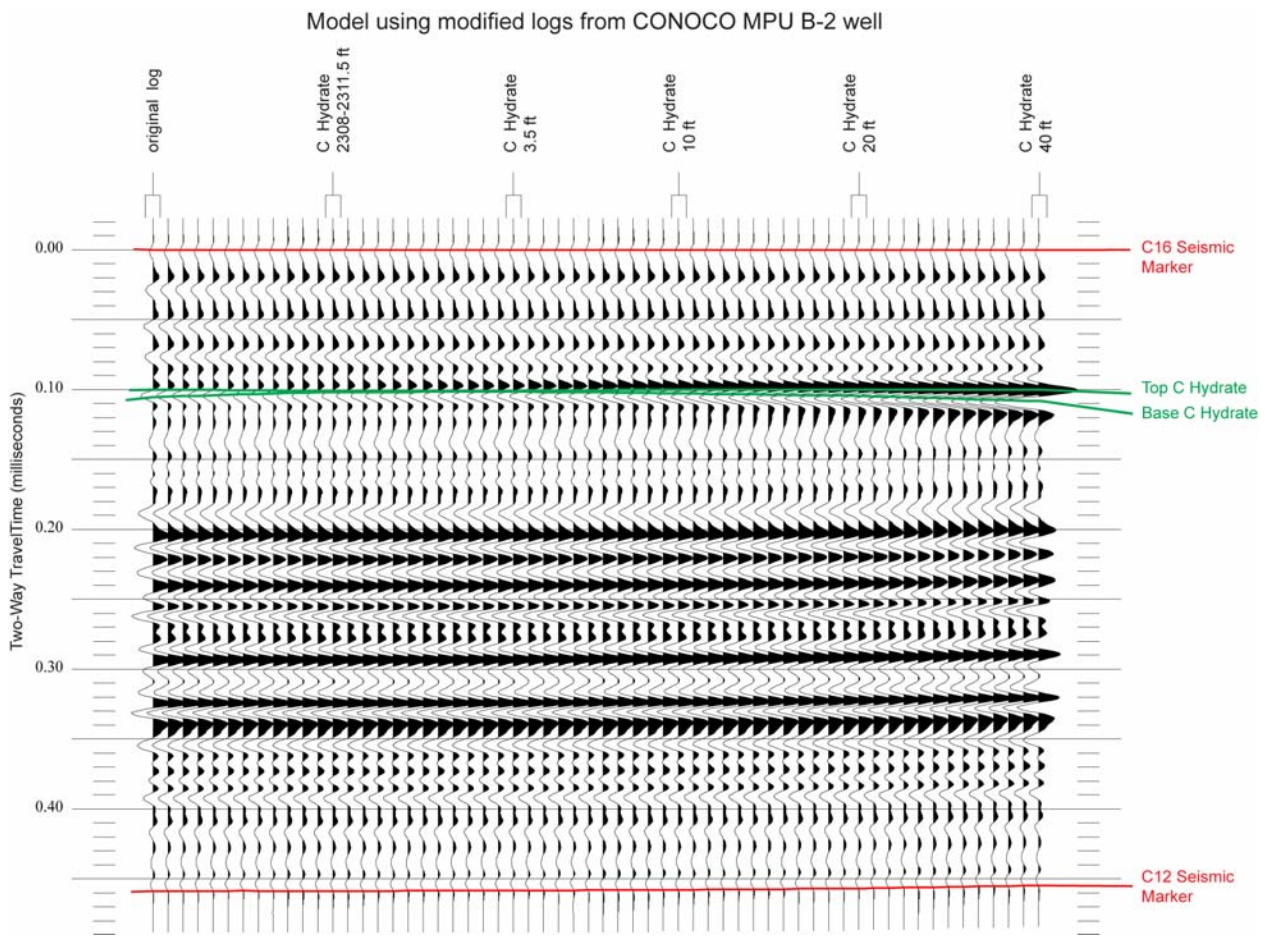


**Figure 10.** This model shows the seismic response to increasing hydrate thickness. Gas hydrate sections greater than about 20 ft thick show an obvious amplitude increase at the Top C Hydrate and Base C Hydrate with all other events remaining constant.

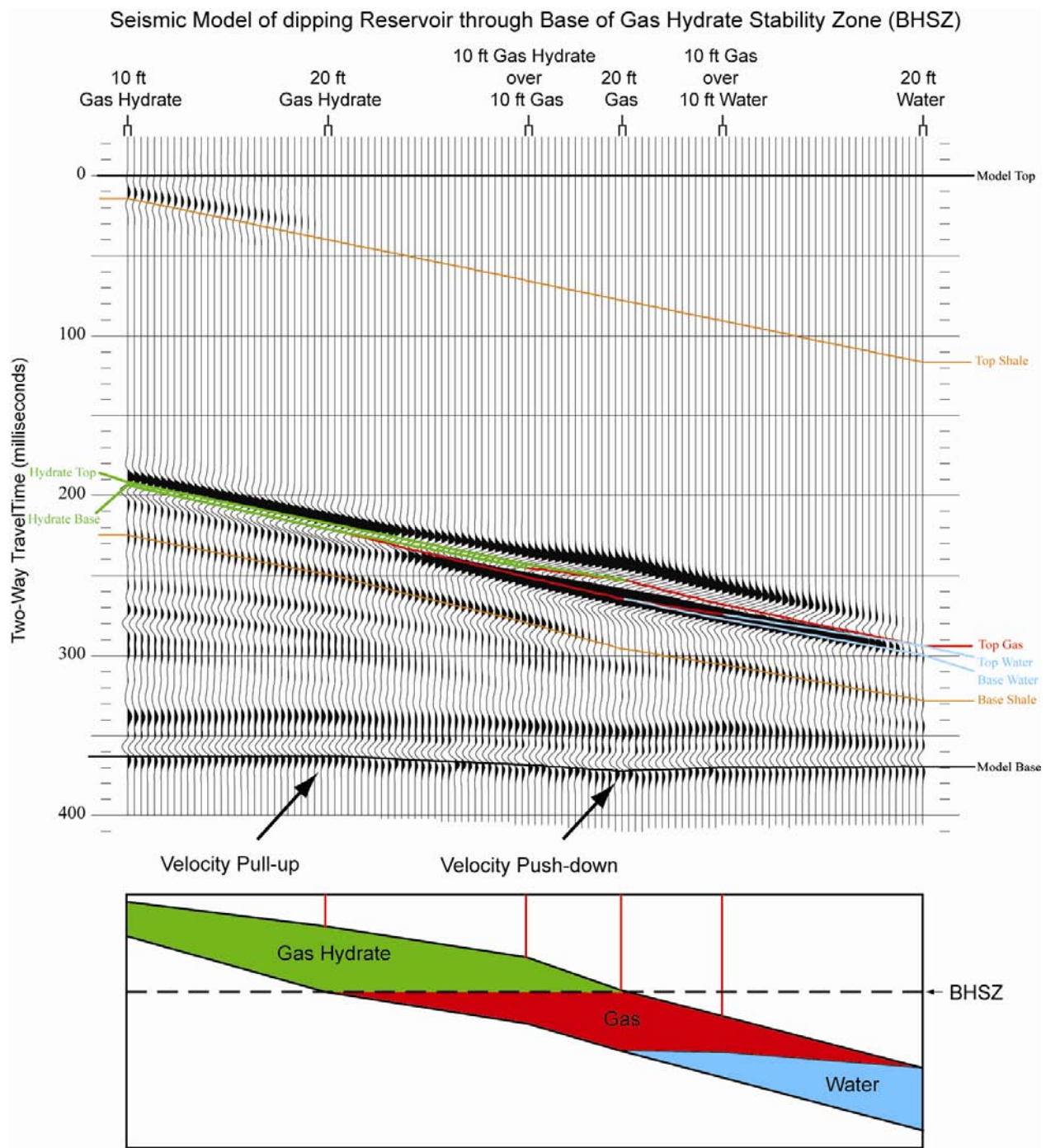


**Figure 11.** This model shows the trace response to a dipping model, at normal SEG polarity. The thin-bed response shows a phase change and amplitude change that is very similar to the actual seismic events near the Base Hydrate Stability Zone (BHSZ). The thick hydrate shows a pull-up and the gas a push-down on the flat model base related to velocity within the reservoir interval.

## Petrophysical Analysis

Petrophysical analysis of available well logs provided further verification and calibration of the seismic attributes suggested by the modeling and also the potential volume of gas hydrates. Analysis provided information about the nature of potential gas hydrate and free gas reservoirs in the section from approximately the middle part of the Staines Tongue of the Saganavirktok Formation (see **Figure 4**) up through the base of the ice bearing permafrost. Analysis produced resistivity log derived water saturation ( $S_w$ ) log curves that show hydrocarbon saturations for both gas hydrates and potential gas reservoirs within the section from the IBPF to near the Top of the Ugnu Sands (Collett, 1993). This analysis required the input of temperature data, pore-water resistivity ( $R_w$ ) data (for salinities ranging from 4 to 10 ppt) and density porosity data. These data were then combined within a standard Archie's calculation of  $S_w$  using Humble constants ( $a=0.62$ ,  $m=2.15$ ). Temperature curves and  $R_w$  curves were calculated for various salinities from the base of IBPF down through the Staines Tongue.

Several wells within the survey area penetrated gas hydrates, as interpreted from wireline log data.  $S_w$  calculations for these thin gas hydrate zones yield a suppressed gas saturation due to degraded well log quality. In the MPU E-26 well, for example, gas hydrate saturations in interpreted C and D hydrates are between 40 % (for  $R_w$  of 4 ppt) and 62% (for  $R_w$  of 10 ppt.) Thin bed modeling shows that these gas hydrates may reach 90% saturation in some of the best prospects with thicker reservoirs.

Well log analysis implied low pore-water salinities in the range of 4 to 6 ppt. Within the Staines Tongue interval, incorrect saturations are calculated within the coals, as Archie's equation does not accurately calculate  $S_w$  for these very low density intervals.  $S_w$  within known gas hydrate intervals based on log analysis (Collett, 1993) shows gas saturations in the range of 91 to 52 % which would be within the range of seismically detectable saturations if reservoir thickness exceeds 25-30 ft.

Shown in **Figure 12** is a log suite from the MPU S-15 well. In this well, the top of the Staines Tongue of the Saganavirktok is well above the Base of the Hydrate Stability Zone. A suite of  $S_w$  curves are shown in column to the right of the lithologic column. The brown  $S_w$  curve corresponds to a salinity of 4 ppt and appears to be the only curve in this interval that correlates to an  $R_w$  baseline. Other  $S_w$  curves, calculated with higher salinities, would put some gas in the entire column, even in the shale sections. A potential gas zone shown in this well has water saturations on the order of 60-70% or equivalent to low gas saturations of 30-40%, which is consistent for most of Milne Point. Coals are also important in the interpretation of gas hydrate or gas in the Staines Tongue interval. It does not appear however, that there are any significant coals above the top of the Staines Tongue of the Saganavirktok. The Staines Tongue coals appear to be relatively uniform in all of the well penetrations across the 3-D survey, and do not appear to be related to anomalies that have been attributed to gas within the Staines interval, as the amplitudes vary regardless of the apparent coal distribution in wells. It is important to note that the interpreted gas seismic anomalies are logically found primarily in current structural highs and amplitudes often diminish along structural contours, which imply gas and associated down-dip water, rather than coal effects.

## BP MPU S-15

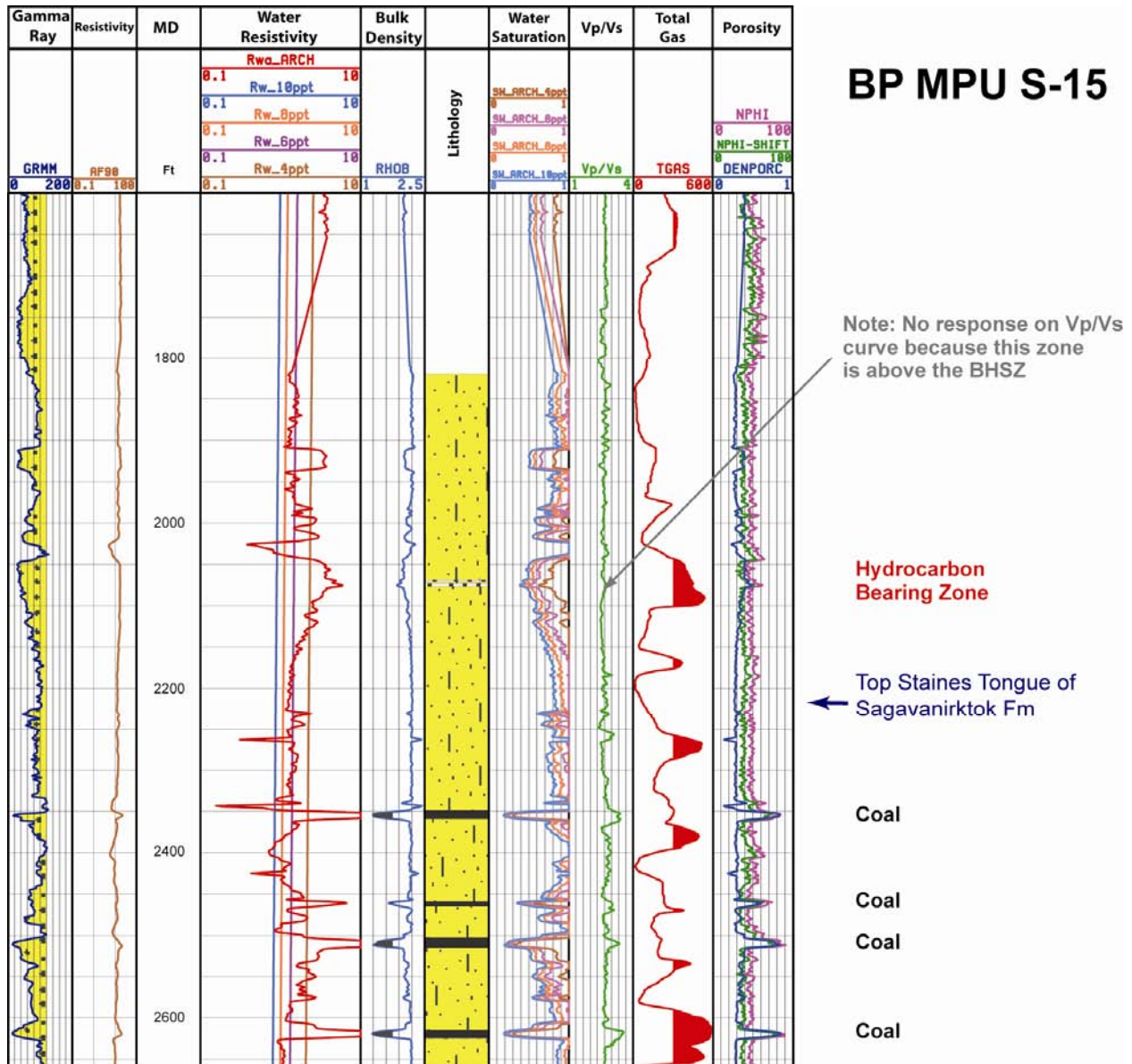
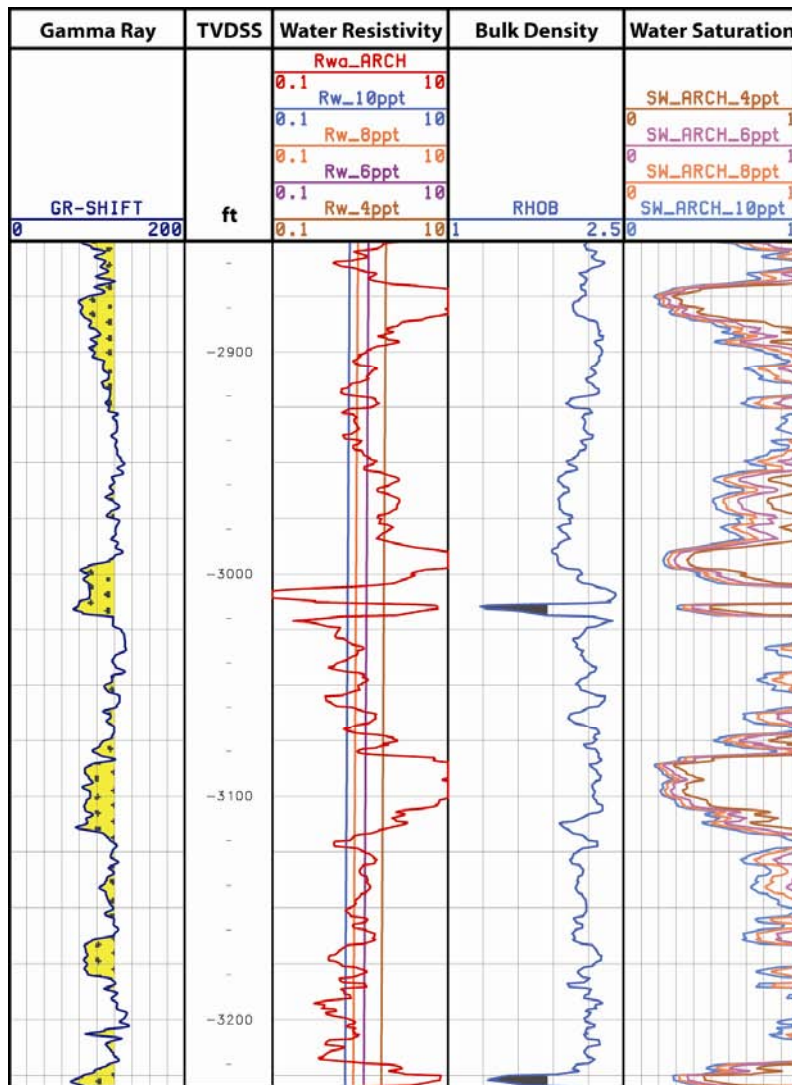


**Figure 12.** The log suite MPU S-15 well is shown with calculated petrophysical curves for water saturation (Sw) and water resistivity (Rw) at various salinities. Coals are found only in the interval below the Top Staines Tongue of the Sagavanirkot in this and other Milne Point wells.

Shown in **Figure 13** is the dramatically different character of the Staines Tongue interval in the Cascade #1 well. This well is in a down-dropped block that is fault separated from the majority of the Milne Point survey. In this well, the high resistivity zones that correspond to gas zones have water saturations of 30-40% corresponding to high gas saturations of 70-80%. This anomalous well is the only one found in the Milne Point area that shows such low water saturations within the Staines Tongue interval and does not necessarily conflict with Collett's (1993) estimates of gas hydrates since none of the wells used in the 1993 study penetrated the Staines Tongue interval in the Cascade area.



## BP CASCADE #1 Rw/Sw Analysis

Top of Staines Gas Zone

Mid-Staines Gas Zone

**Figure 13.** The log suite of the Cascade #1 well is shown with calculated petrophysical curves for water saturation (Sw) and water resistivity (Rw) at various salinities.

## Reflection Coefficient versus Gas Hydrate Saturation

Gas hydrate acoustic modeling by Lee (2006) shows that there is little variation in the reflection coefficient of gas hydrate bearing sediments except in sections with gas hydrate saturations greater than 60%. The use of seismic amplitudes to identify gas hydrates within the defined HSZ will show only highly saturated gas hydrate reservoirs – a natural high-grading process. For the case of a shale section overlying a gas saturated section, the reflection coefficients are three to four times the magnitude of shale over hydrate reservoirs, even at low saturations. Thus, the average amplitude below the BHSZ, is likely to be higher than that of the Gas Hydrate Stability Zone even if small amounts of gas are present.

Shown in **Figure 14** is an example reflection strength display from the Milne Point 3-D survey. The minimum and maximum depths for the Base Gas Hydrate Stability Zone (BHSZ) are shown as parallel green and yellow lines on the display. Notice that, as expected, the interval above the BHSZ is nearly reflectionless, while high amplitude events are obvious below the BHSZ. The high amplitude events below the BHSZ, in several cases, appear to end at the BHSZ. These are interpreted to be free gas bearing sediments that are trapped by thin (or low saturation) gas hydrate at the BHSZ. The amplitude of these events does not provide insight into the gas saturation of the units.

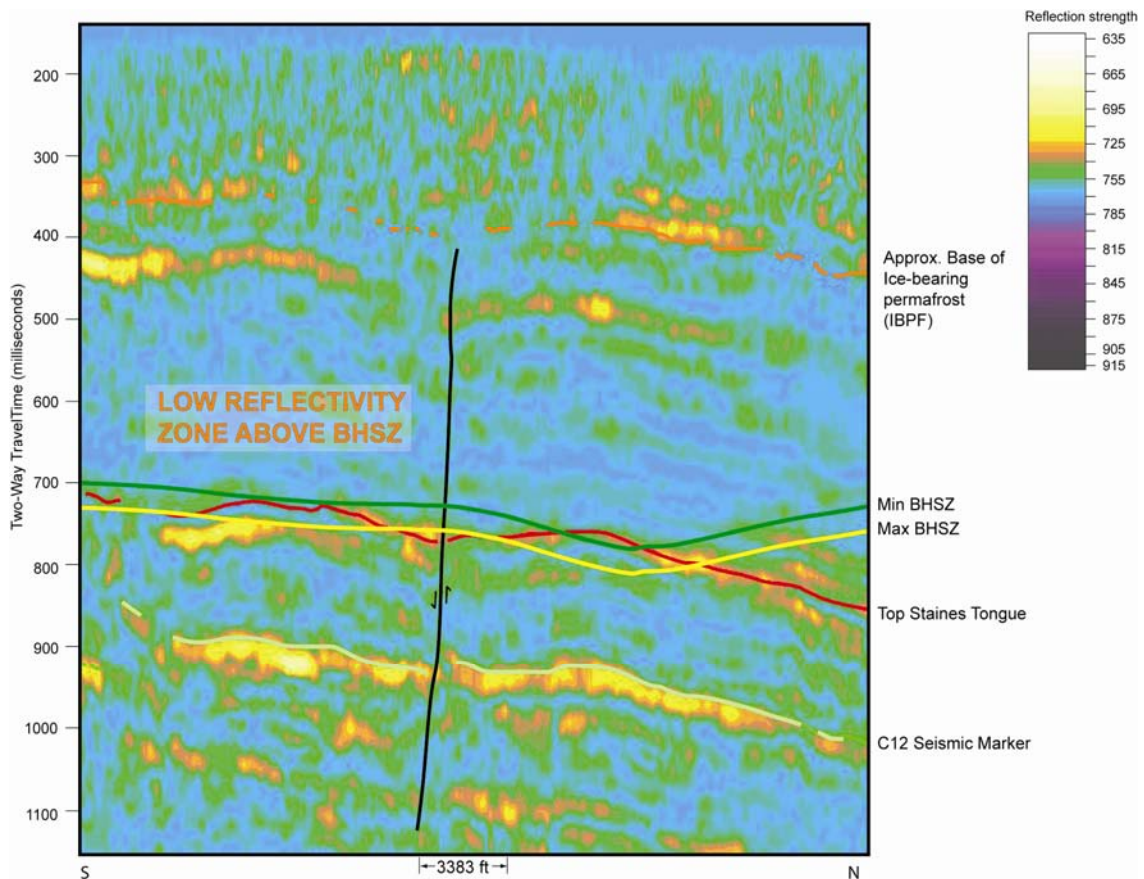


**Figure 14.** This seismic display is a line from a reflection strength volume. Parallel green and yellow lines depict the margin of error in the calculated Base Hydrate Stability Zone (BHSZ, from log data.).

## *Seismic Stratigraphic Correlation*

Several historical log correlations were shown to be excellent seismic markers within the Milne Point 3-D survey. The C16 Seismic Marker and the C12 Seismic Marker shown in **Figure 15** are easily interpreted across the whole survey. The C16 seismic marker is generally below the IBPF, and the C12 Seismic Marker is below the BHSZ everywhere on the 3-D survey. The Top Staines Tongue of the Saganavirktok is also an interpretable event across the 3-D survey, and is very near the BHSZ over most of the area.

The shallowest interpreted horizon is the Top Mikkelson which is above the IBPF and is often disrupted by data problems in the near surface. The Top Mikkelson to C16 seismic marker bracket a significant regional unconformity that causes thinning of the Saganavirktok section from the East to the West. The IBPF may be a strong reflector in certain parts of the survey, but strong reflections from gas hydrates, which may be co-mingled with permafrost make direct interpretation of the IBPF from seismic unreliable. Few continuous events can be interpreted within the Gas Hydrate Stability Zone other than the C16 Seismic Marker and various events that have been correlated to gas hydrate reservoir intervals. The C12 Seismic Marker appears correlate to a regionally continuous coaly interval below the Staines Tongue of the Saganavirktok.

The West Sak 25 and the MPU S-15i were found to be problematic due to the fact that the base of IBPF was difficult to pick because gas hydrates were co-mingled with permafrost. The base of IBPF picks were re-adjusted for these two wells based primarily on analysis of seismic amplitudes. From these re-adjusted picks, new BHSZ values were calculated and a new BHSZ horizon was generated. A pair of horizons was then generated representing the upper and lower limits of the base of the BHSZ with an error range of plus or minus 75 ft. (+/- 15 ms) and are shown in **Figure 15** as the parallel green and orange lines. Note that in this case, high amplitude events truncate or diminish in amplitude very near the minimum BHSZ, probably indicating the expected transition from free-gas to gas hydrate as predicted in the modeling.

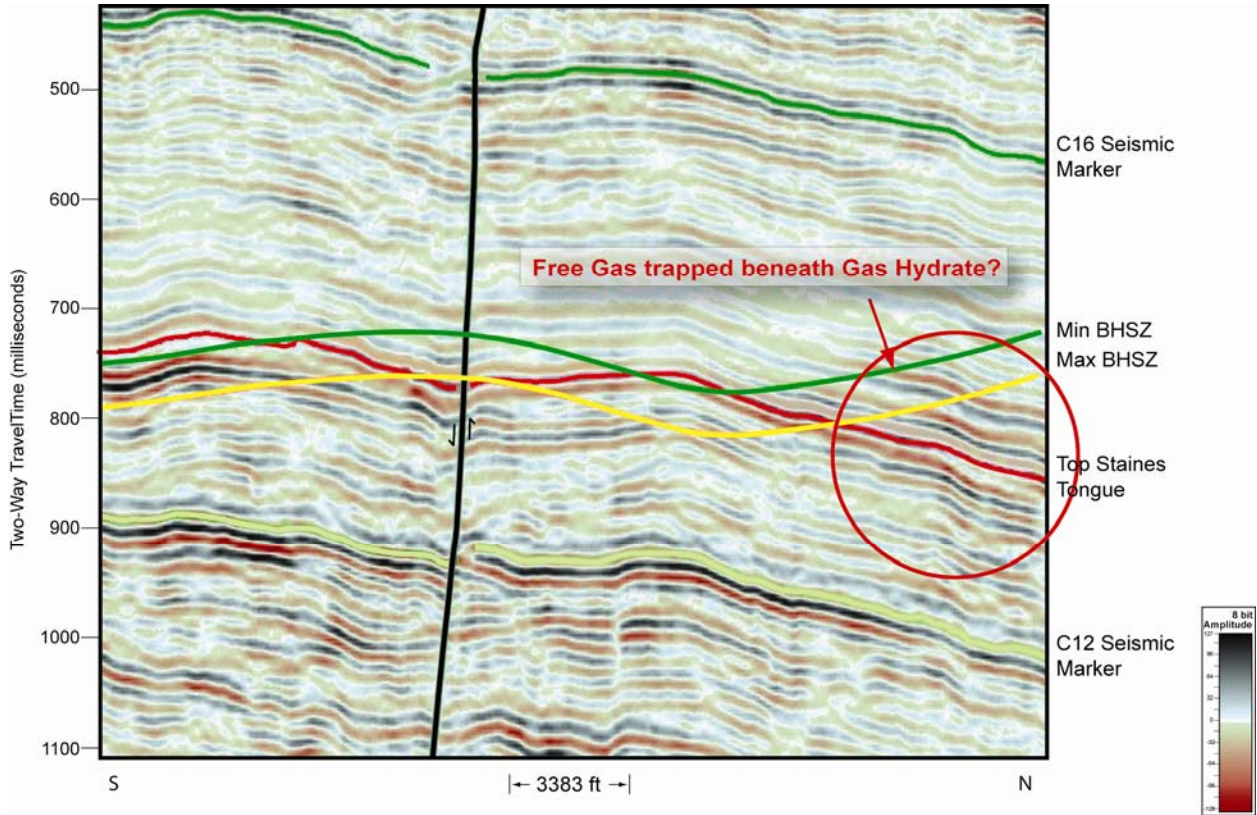


**Figure 15.** This seismic line is a color variable density display from the amplitude volume. The zone of interest is between the C16 Seismic marker (dark green) and the parallel green and yellow lines which represent the margin of error for the Base Gas Hydrate Stability Zone (BHSZ) horizon. The abrupt terminations of amplitude near the minimum base of the Hydrate Stability Zone (Min BHSZ) are interpreted as gas trapped by the hydrate.

## **PROSPECTING**

“Intra-Hydrate” prospecting depended primarily on seismic character analysis and correlation with well log responses. The results of rock physics modeling and trace modeling showed expected seismic attributes for various intra-Hydrate Stability Zone scenarios. As shown previously in this paper and in Lee et al. (in press), seismic frequencies limited intra-gas-Hydrate Stability Zone prospect identification to those meeting a minimum criterion of >25 ft thickness and > 60% gas hydrate saturation with the attributes developed to-date. These prospects are defined within the standardized “Eileen” gas hydrate accumulation nomenclature as belonging to the A through E Hydrate Units (Collett, 1993) shown in **Figure 16**. Current production modeling assigns those closest to the Base Hydrate Stability Zone, A and B, as those that would be the most producible, with the D and E hydrates being more difficult to produce and complicated by their proximity to the permafrost in this area. Regionally interpreted seismic stratigraphic events were correlated to the Mikkelsen Tongue, the C16 event, the top of the Staines Tongue, and the C12 event. Within this framework, the occurrence of gas hydrate was interpreted utilizing observations from detailed log analysis by Lee (2006). The log analysis pointed to several key criterions that could be used in seismic interpretation to identify gas hydrate or sub-hydrate gas.

The focus of the project centered on the interval below the base of ice bearing permafrost (IBPF) to just below the base of Gas Hydrate Stability Zone. Shown in **Figure 16** are the known regional gas hydrate occurrences. The Milne Point work has confirmed the stratigraphic consistencies of this correlation into the Milne Point study area. Known gas hydrates in wells within the Milne Point 3-D survey have been correlated both seismically and stratigraphically using well logs.

Gas hydrate reservoirs below the IBPF and within the Hydrate Stability Zone (Intra-Hydrate) have acoustic properties allowing them to be identified by several simple seismic attributes. Several candidates for “Intra-Hydrate” prospects were found during reconnaissance mapping of this interval as shown in **Figure 17**. Average maximum amplitude was extracted from the 3-D seismic for an interval from 50 ms below the C16 Seismic Marker to 50 ms above the Staines Tongue marker.

Regional correlations of the top of the Mikkelsen Tongue, the C16 seismic marker, the top of the Staines Tongue, and the C12 seismic marker and several regional markers within the interval below the Canning were the primary seismic events used in this study as previously discussed. Reconnaissance of the interval from the C16 seismic marker to the BHSZ showed promising areas for gas hydrate prospecting based on amplitude analysis of the true amplitude volume. The map shown in **Figure 18** shows areas of higher amplitude within the HSZ which would be expected to be gas hydrate bearing based on seismic modeling.

The similarity in acoustic properties between ice and gas hydrate makes it difficult to differentiate between ice- and gas-hydrate-bearing sediments. Therefore gas hydrates adjacent to permafrost, while prospective, are difficult to quantify and produce (Collett, 2002). In the Milne Point 3-D area, some assumptions can be made to constrain modeled results describing the relationship of these boundaries in the stack and offset domains. First, if we can assume that thermogenic gasses migrated into what are now fully saturated gas hydrate reservoirs we could

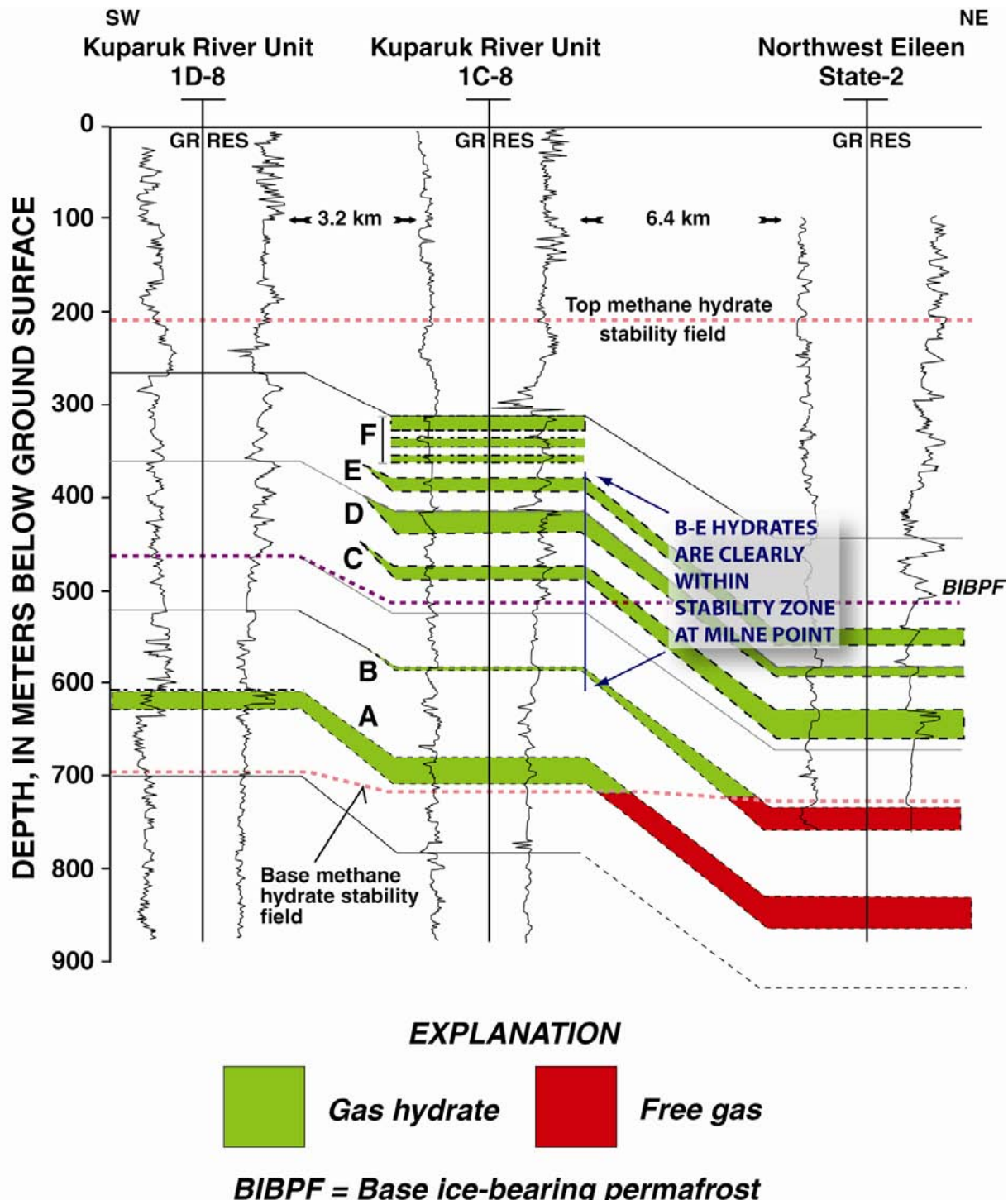


**Figure 16.** The Eileen gas hydrate correlations from Collett (1993). The “B” through “E” Gas Hydrate Units are within the Hydrate Stability Zone at Milne Point. “E” and “D” gas hydrate units are commingled with permafrost in some parts of Milne Point.

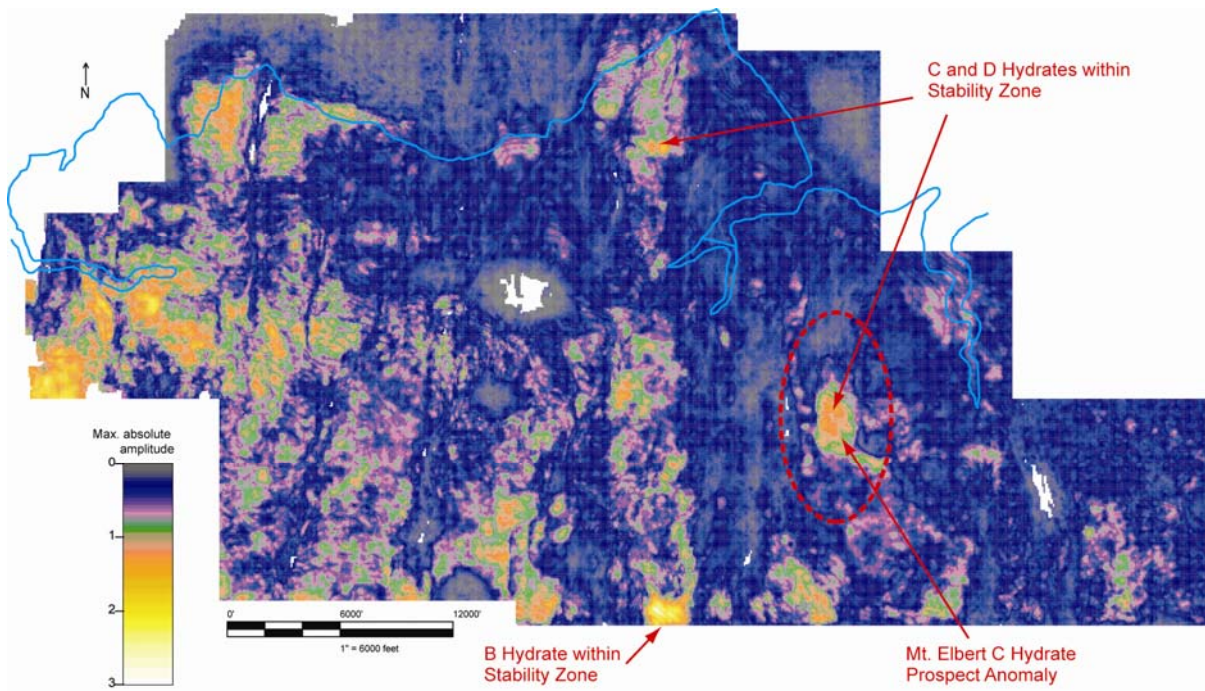


**Figure 17.** The Intra-Hydrate prospect reconnaissance map within the Gas Hydrate Stability Zone shows the Maximum absolute amplitude from 50 ms below the C16 Seismic Marker to 50 ms. above the Upper Staines Tongue Marker. Several areas of interest were identified, including the Mt. Elbert “C” hydrate anomaly.

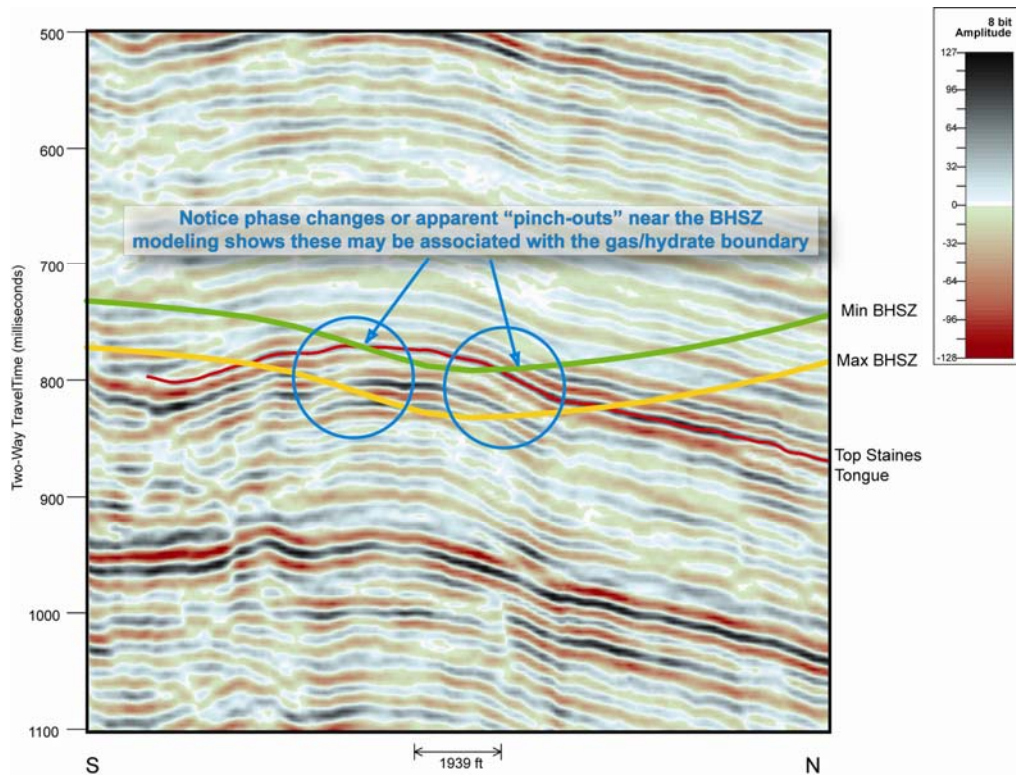


**Figure 18.** The minimum and maximum Base Hydrate Stability Zone events are shown relative to truncated high amplitude seismic reflections that are interpreted to be sub-hydrate free gas accumulations.

assume a gas hydrate concentration in sandstone reservoir rock of about 80 to 85% – similar to conventional gas reservoirs. Unconsolidated sandstone reservoirs in the Sagavanirktok Formation that contain the majority of Milne Point gas hydrates typically have 30-40% porosity. Reservoir thickness is the main variable used in modeling acoustic attributes and in calculating volumetrics.

Free-gas prospects that are associated with the BHSZ represent the second type of target for our prospecting effort (**Figure 18**). Our work shows that there is a predictable relationship between the BHSZ and amplitude anomalies thought to represent free gas. Initially, the BP Cascade-1 well in the far southeast portion of the 3-D survey was thought to show an example of a sub-hydrate trapped free-gas column. In the well, a 300-ft-thick free-gas accumulation exists in an excellent reservoir interval within the zone mapped as the Staines Tongue of the Sagavanirktok Formation (approximately the C13 zone.) Northwest of the Cascade block however, the same reservoir interval displays high amplitudes typical of a gas charged reservoir directly below the interface between the Gas Hydrate Stability Zone.

Free gas trapped below gas hydrates or below the Gas Hydrate Stability Zone (Sub-Hydrate) can be easily identified by seismic attributes in this geologic setting, however low saturation gas can give nearly the same acoustic signature as higher saturation gas reservoirs. It can be shown that the seismic amplitude anomalies are associated with free gas at the Base Hydrate Stability Zone, and are connected to up-dip gas hydrate reservoirs. In some cases, no distinct amplitude anomalies attributed to gas hydrates above the free-gas to gas-hydrate boundary have been identified, even though convention would indicate that gas-hydrates must be present to form the trap. These free gas accumulations are also potentially prospective as exploration targets, but in this area, are low saturation targets that help identify the BHSZ.

Only larger regional faults that were recognized as potential migration pathways were interpreted in the deeper producing zone below the Canning Shale. The subsurface geology in the Milne Point 3-D seismic survey area shows that the gas hydrate-bearing zone is separated from the Kuparuk and older Ellesmerian section by the Canning Shale. The few faults that originated in the Ellesmerian section, that pass through the Kuparuk River Formation and the shale zone terminating in the gas hydrate-bearing section most likely acted as conduits for deep free gas to migrate into the Gas Hydrate Stability Zone, and supplying the gas that transformed into gas hydrate. **Figure 19** shows a vertical seismic view depicting how the weak amplitude Canning Shale zone separates the deep, higher amplitude Ellesmerian-Kuparuk section from the shallow high amplitude gas hydrate-bearing Sagavanerktok section. Also note in **Figure 19** the interpreted faults and how the majority of them die in the shale zone, yet some of the larger regional deep seated faults can pass through the shale zone into the gas hydrate-bearing Sagavanirktok section above.

Two distinct sets of fault orientations were identified in the interpretation. A deep seated fault pattern, predominantly northwest to southeast with a conjugate set of faults running southwest to northeast can be seen in the deep Ellesmerian section up through the Kuparuk Fm. Above the shale section of the Canning Formation the faults strike predominantly north-south with a minor conjugate set running northwest to southeast. The north-south trending faults can be seen above the shale zone through the gas hydrate-bearing zone almost to the surface while the conjugate

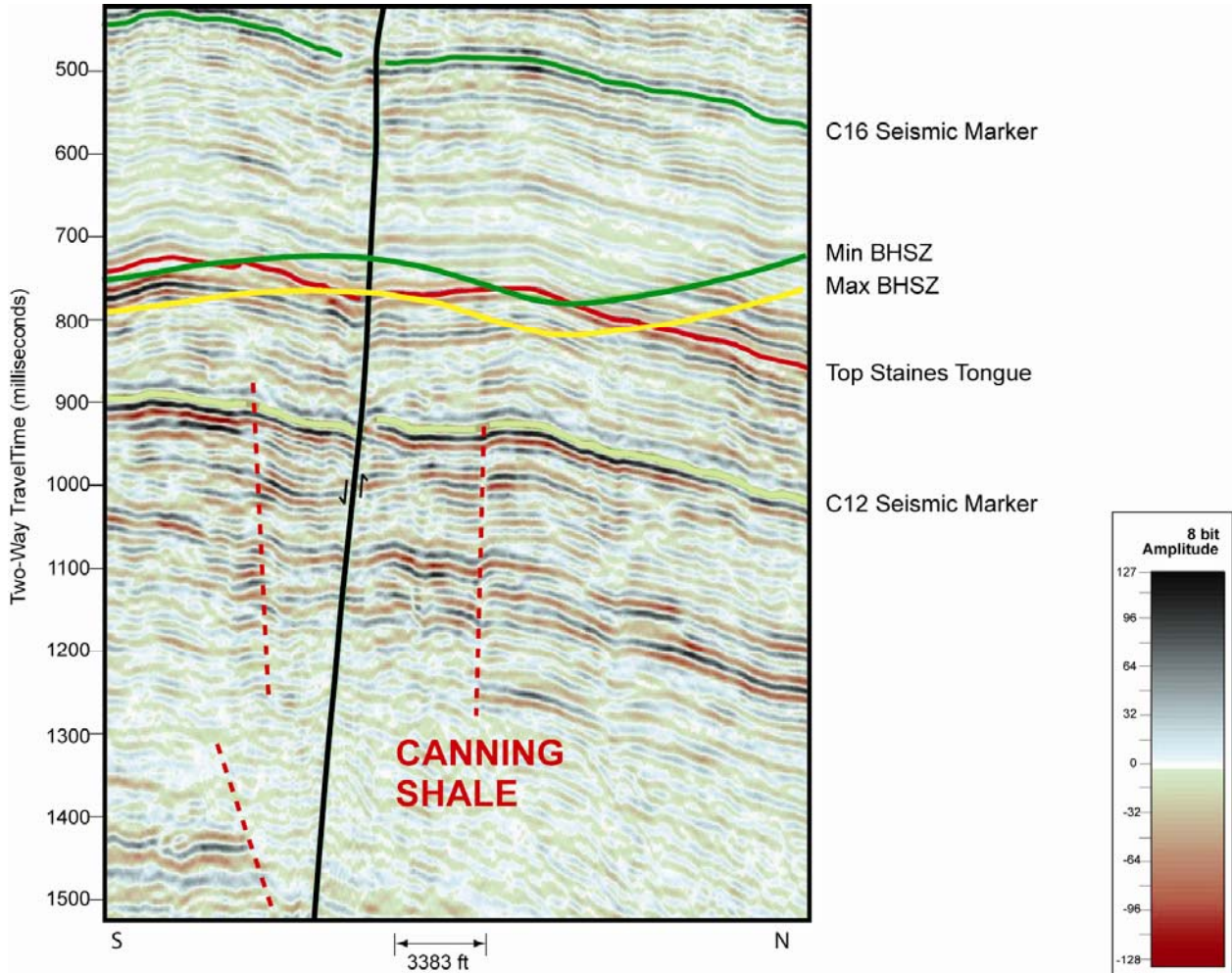


**Figure 19.** This seismic line shows the thick, nearly reflectionless, Canning Shale zone separating the Hydrate Stability Zone interval from the deeper Ellesmarian section that produces oil and gas in Milne Point, Kuparuk River and Prudhoe Bay fields. Some larger regional faults can be seen cutting this interval.

fault set dies out within the Saganavirktok section. The shale zone appears to separate faults that were formed under two slightly different stress regimes. Since there are only a few good coherent reflections in the shale zone it is hard to determine which of the deep seated faults were through-going into the gas hydrate-bearing zone, however some of the largest regional faults within the deep section were interpreted as through-going faults. Shown in **Figure 20** is an interpreted timeslice at 700 ms, near the IBPF. It has been hypothesized that the SW to NE trending faults that are more similar to the deep faulting may be more likely to be connected to the deeper hydrocarbon system below the Canning. These faults may more likely provide paths for sourcing the shallower free gas reservoirs and gas hydrate reservoirs.

Proper interpretation of the faults in the Milne Point 3-D seismic survey area played a large role in defining the compartmentalization of the gas hydrate and gas prospects interpreted in this project. Particular attention was taken in developing a geologically sound fault interpretation but certain geophysical conditions such as phase reversals and velocity pull-ups associated with gas hydrate accumulations may appear similar to faulting on the seismic data.

From the analysis of the seismic data, several intra-gas-Hydrate Stability Zone prospects have been identified in the Milne Point 3-D survey area. Intra-gas-hydrate prospects are typically fault bounded and are identified primarily by their acoustic properties (see Lee et al, in press). As a rule, areas that are currently structurally high within prospective fault blocks can be shown to have acoustic properties that correspond to higher concentrations of gas-hydrate. This structural relationship is similar to conventional gas prospects, pointing back to the free-gas origin of these gas hydrates. It is also clear that some of these fault blocks do not appear to be “fully charged”, as there are down-dip limits to the mapped acoustic anomalies. Several of these intra- gas hydrate prospects appear to be candidates for gas-hydrate production testing, due to their proximity to existing roads and infrastructure.

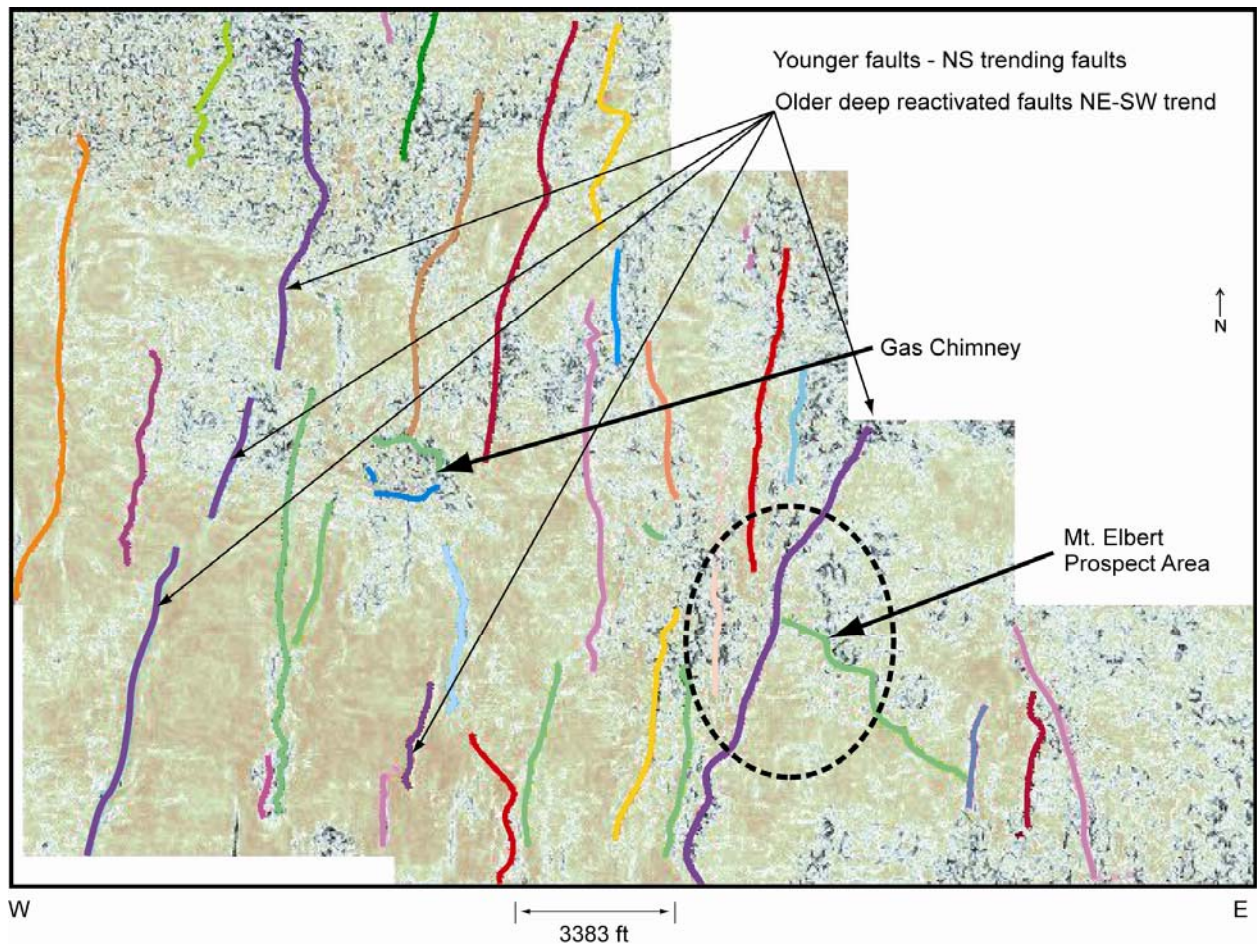


**Figure 20.** This display shows a shallow coherency timeslice with various fault trends. Older faults, trending more NE to SW, are more likely to be conduits for hydrocarbon migration.

## Intra Gas Hydrate Prospects

A series of 14 intra-gas hydrate (Intra-Hydrate) prospects were identified that met the minimum thickness and saturation criterion. The map in **Figure 21** shows the outline of the Milne Point gas hydrate prospects. The outlines represent the aerial distribution of seismic amplitudes attributed to gas hydrate, color coded by prospective interval within the Gas Hydrate Stability Zone. In this display, light green represents “A”, pink represents “B”, yellow represents “C”, blue represents “D” and gold represents “E” gas hydrate prospects. The dark green outlines show Mid-Staines-gas hydrate. Staines gas hydrate prospects are associated with the base of the hydrate stability field in the Milne point area and are not discussed further in this paper. These prospects were further analyzed to compute volumetrics, using a Monte Carlo routine to compare reservoir physical properties. **Table 2** summarizes the intra-gas hydrate prospects. The Mt. Elbert prospect stands out due to its aerial size and potential for multiple pay zones. The Mt. Elbert prospect is the best defined of the intra-gas hydrate prospects identified in this study and is in close proximity to existing infrastructure.

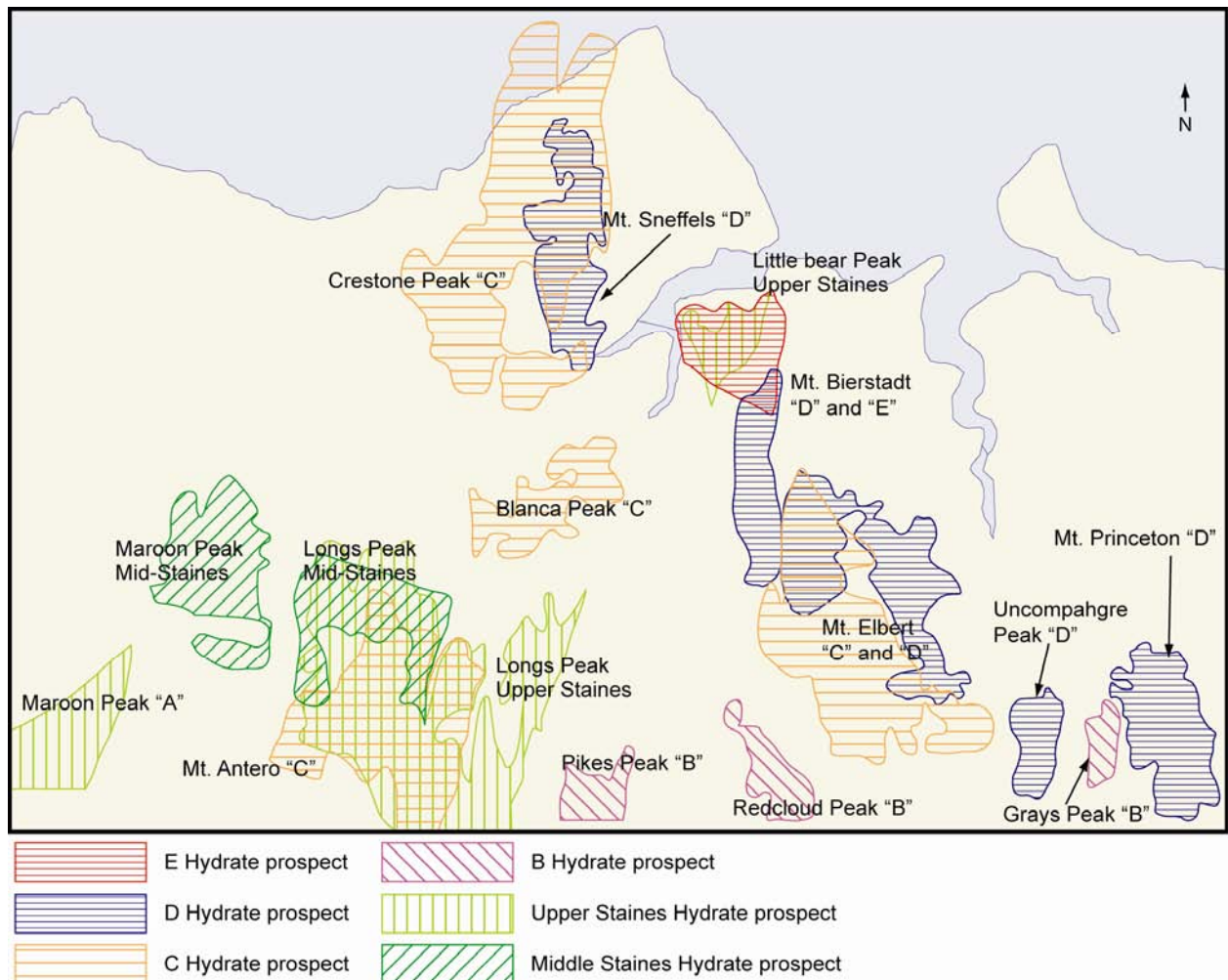


**Figure 21.** This display shows Milne Point gas hydrate prospects developed by 3D seismic analysis.

Prospect Names	Zone	closure sq.mi	closure acres
<b>Intra-Hydrate Prospects</b>			
Mt. Bierstadt "E" Hydrate Prospect	E	0.52	332
Mt. Elbert "D" Hydrate Prospect	D	0.42	267
Mt. Bierstadt "D" Hydrate Prospect	D	0.42	268
Mt. Sneffels "D" Hydrate Prospect	D	0.8	516
Uncompahgre Peak "D" Hydrate Prospect	D	0.26	167
Mt. Princeton "D" Prospect	D	0.7	449
Crestone Peak "C" Hydrate Prospect	C	2.7	1728
Mt. Antero "C" Hydrate Prospect	C	1.49	955
Mt. Elbert "C" Hydrate Prospect	C	1.69	1106
Blanca Peak "C" Hydrate Prospect	C	0.51	328
Pikes Peak "B" Hydrate Prospect	B	0.46	298
Redcloud Peak "B" Hydrate Prospect	B	0.3	194
Grays Peak "B" Hydrate Prospect	B	0.13	85
Maroon Peak "A" Hydrate Prospect	A	0.58	375

**Table 2.** Summary of intra-gas hydrate prospects identified using the Milne Point 3-D seismic survey.

Calculation of saturation and thickness for intra-hydrate prospects on the Milne 3-D survey utilize a “thin-bed” modeling approach described by Lee et al (in press). Modeling, based on a dominant seismic frequency of 55 hz., shows that for all thicknesses within the expected reservoir thickness range from 1 to 100 ft, gas hydrate saturated reservoirs are seismically transparent for zones with gas saturations less than 40%. Similarly, there is no seismic response to gas hydrate reservoirs less than a cut-off thickness of 25 – 30 ft.

The Lee et al (in press) assumptions work well for isolated gas hydrate bearing reservoirs within the HSZ. However, for gas hydrates that are adjacent to free gas reservoirs at the base of the Hydrate Stability Zone, these assumptions may not apply. In the case of combined gas hydrate and free gas reservoirs, modeling shows that the acoustic effect of the gas is likely to be much larger than that of a comparable gas hydrate in the same reservoir. Constructive and destructive interference are likely to occur in areas of overlap. Also, if thin gas hydrate reservoirs are stacked above gas reservoirs within reservoirs near the BHSZ, constructive and destructive interference will make “thin bed” analysis invalid. In these cases, we rely on well analogs and regional log analysis to choose our parameters for volumetric evaluation.

A representative intra-hydrate prospect, the Mt. Elbert Prospect, with interpreted “C” and “D” gas hydrate units is shown on the seismic section in **Figure 22**. Note that the interpreted events are higher amplitude than the typical background amplitude of the HSZ shown by the red arrow. The high amplitude events correlate to weaker events at the well where thin “C” and “D” gas hydrates have been identified on logs. **Figure 23** shows a three dimensional display of fault bounded amplitude on structure for the Mt. Elbert “C” gas hydrate prospect. The thin gas hydrates at the E-26 well are below the 25 ft minimum thickness required for identification of gas hydrates using the seismic data. For thin-bed modeling, the amplitude of the “C” gas hydrate event (a trough on this reverse polarity data) and the adjacent peak, below the “C” gas hydrate event were extracted from the true amplitude processed 32 bit data.

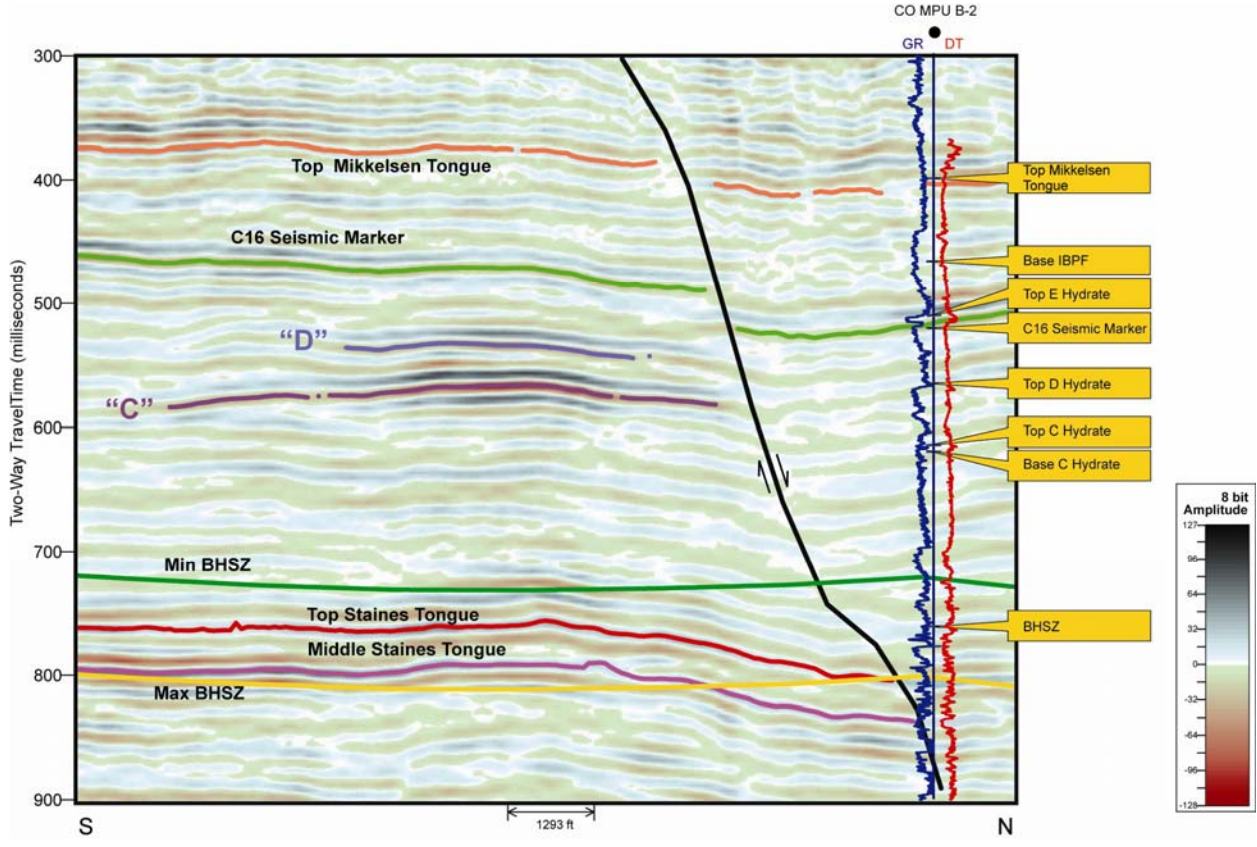


**Figure 22.** The CO MPU B-2 well tie, down-dip of Mt. Elbert C and D hydrate anomalies show thin hydrates identified on logs. These hydrates are below the detection limits of the seismic (less than 25 ft thick.) Amplitude anomalies in the up-thrown block correlate to these hydrates and are interpreted to be thicker, high saturation hydrates.

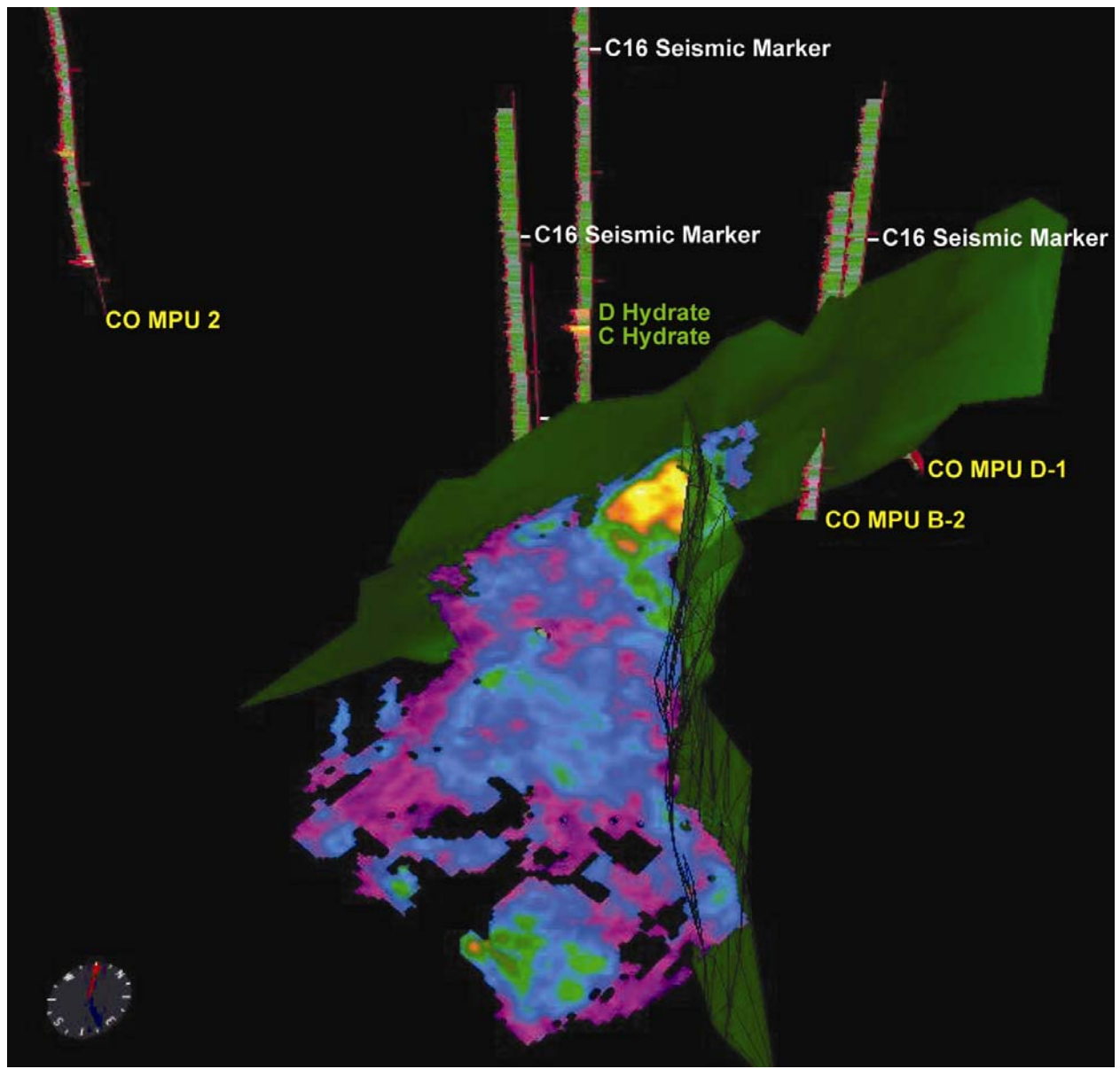


**Figure 23.** This 3-D display of the fault bounded Mt. Elbert prospect amplitude horizon shows the relationship of the anomaly to bounding faults and wells.

Intra-Hydrate Stability Zone anomalies attributed to gas hydrate were interpreted as troughs since the data were acquired in reverse polarity. Shown in **Figure 24** is a representative seismic line that displays the response of both gas hydrate and free gas in the same stratigraphic interval on either side of a significant normal fault. The gas, below the BHSZ is clearly weighted as a peak, and the gas hydrate section above the BHSZ is shown as a trough.

The 55 Hz dominant frequency was calculated from a power spectrum of the data over the zone of interest. This power spectrum is typical of any taken from the survey except where the survey goes into the offshore. For the purpose of thickness and gas saturation calculation via the Lee et al (in press) thin bed model, the isochron of the wavelet from trough to peak was calculated, and amplitude extractions were made from both (using the 16 bit “true amplitude” wavelet processed volume.)

As described in Lee et al (in press), reflectivity versus interval travel time between the “C” horizon and the “C Base Event” horizon were plotted as shown in **Figure 25**. The data limits for these frequencies are clearly supporting our previous assumption of approximately 25 ft for our detection threshold. Based on the relationship shown, reservoir thickness and saturation can be estimated according to the algorithms described in Lee et al (in press).

Thickness and gas hydrate saturation attributes were calculated and mapped for the Mt Elbert prospect (Lee et., in press). Shown in **Figures 26 and 27** below, are thickness and saturation maps for the seismic inferred Mt. Elbert prospect. In general, the area mapped as the thickest reservoir corresponds to the area with the highest gas hydrate saturation, and probably not coincidentally, is also primarily on the highest structural part of the fault block. This feature also has a computed thicker section with gas hydrate section relative to the rest of the fault block.

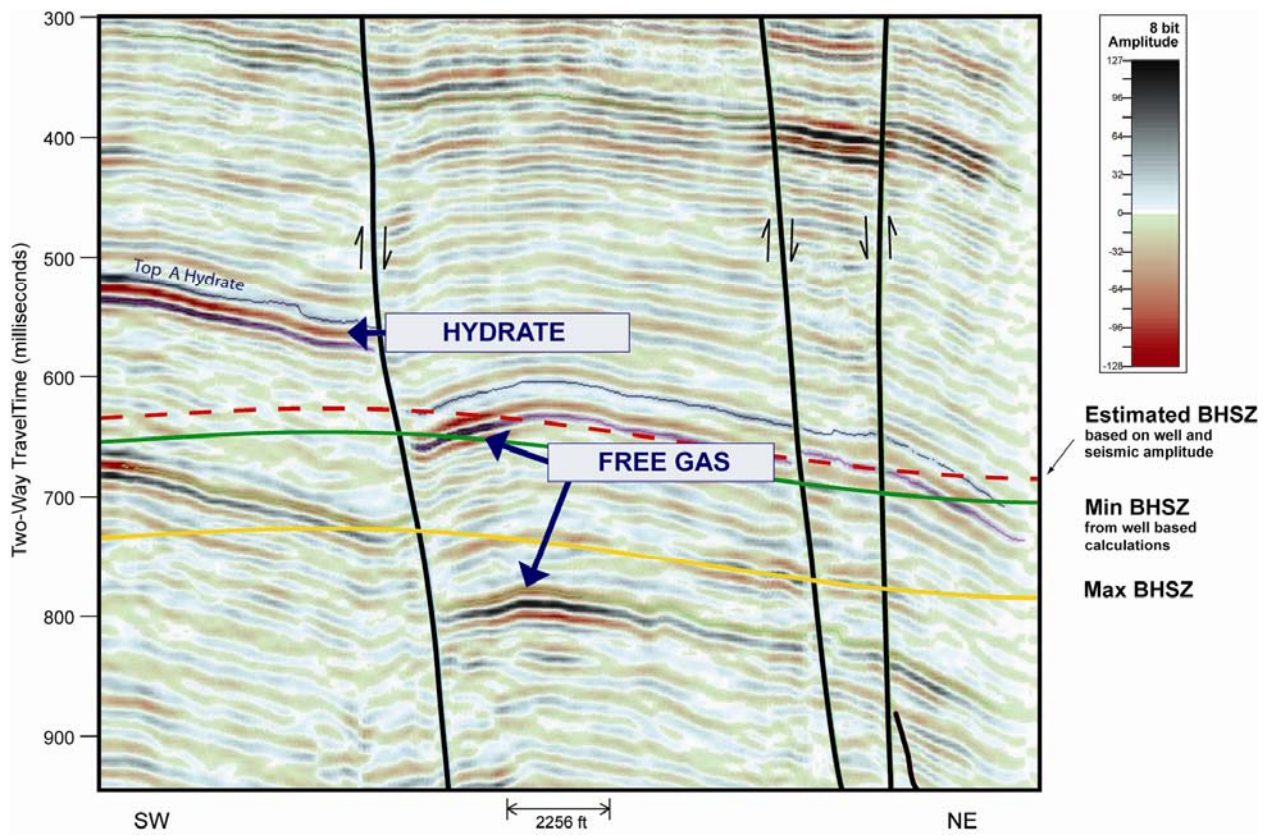


**Figure 24.** The Maroon Peak free gas and gas hydrate prospects are shown by amplitude and phase variations. The “Free Gas” anomalies are represented by a peak, and the “Hydrate” in the up-thrown block is represented by a trough on this reverse SEG polarity data.

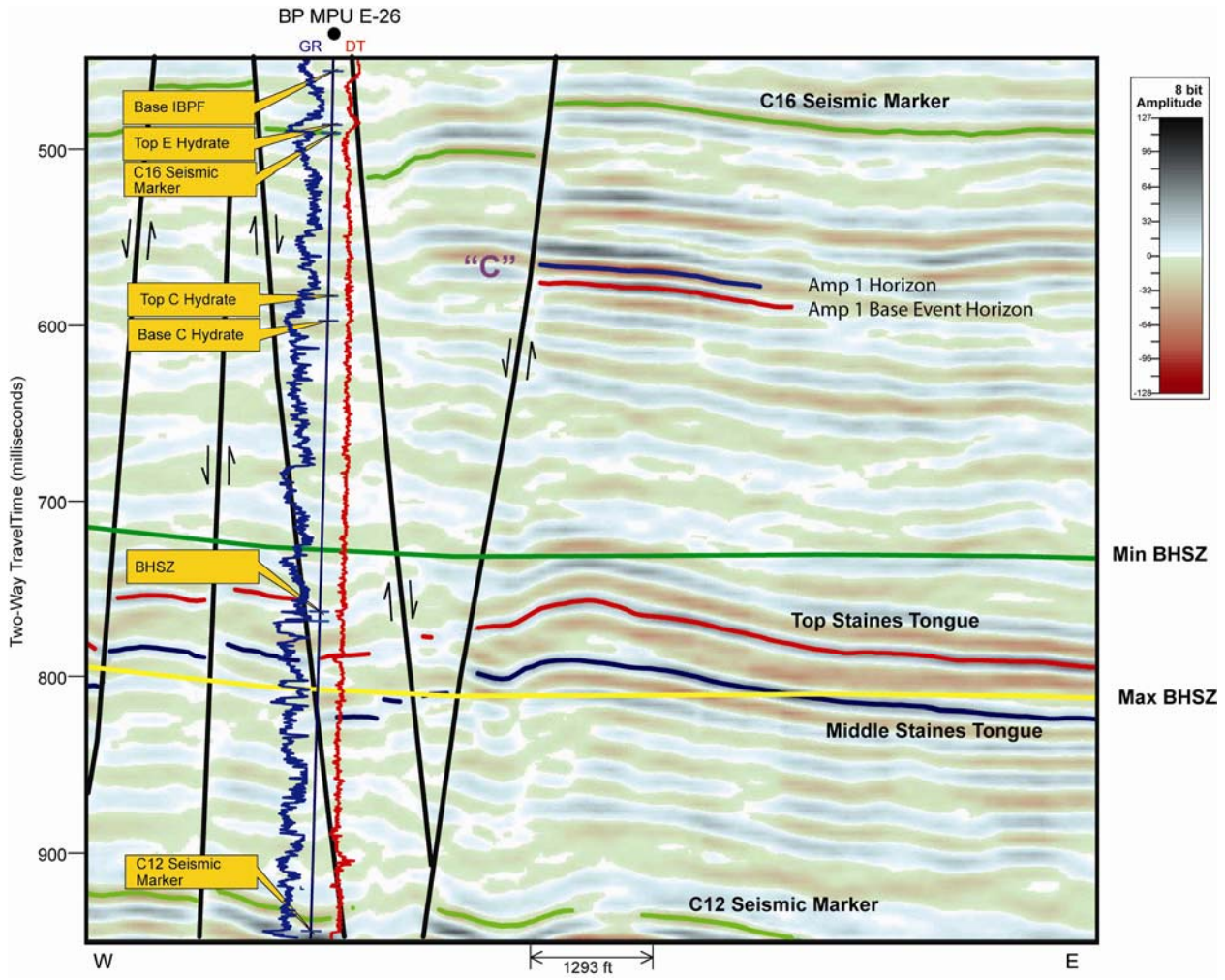


**Figure 25.** This display shows the Mt. Elbert “C” Hydrate events used in Lee’s saturation calculation. The Seismic line shows the tie across the fault to the BP MPU E-26 well.

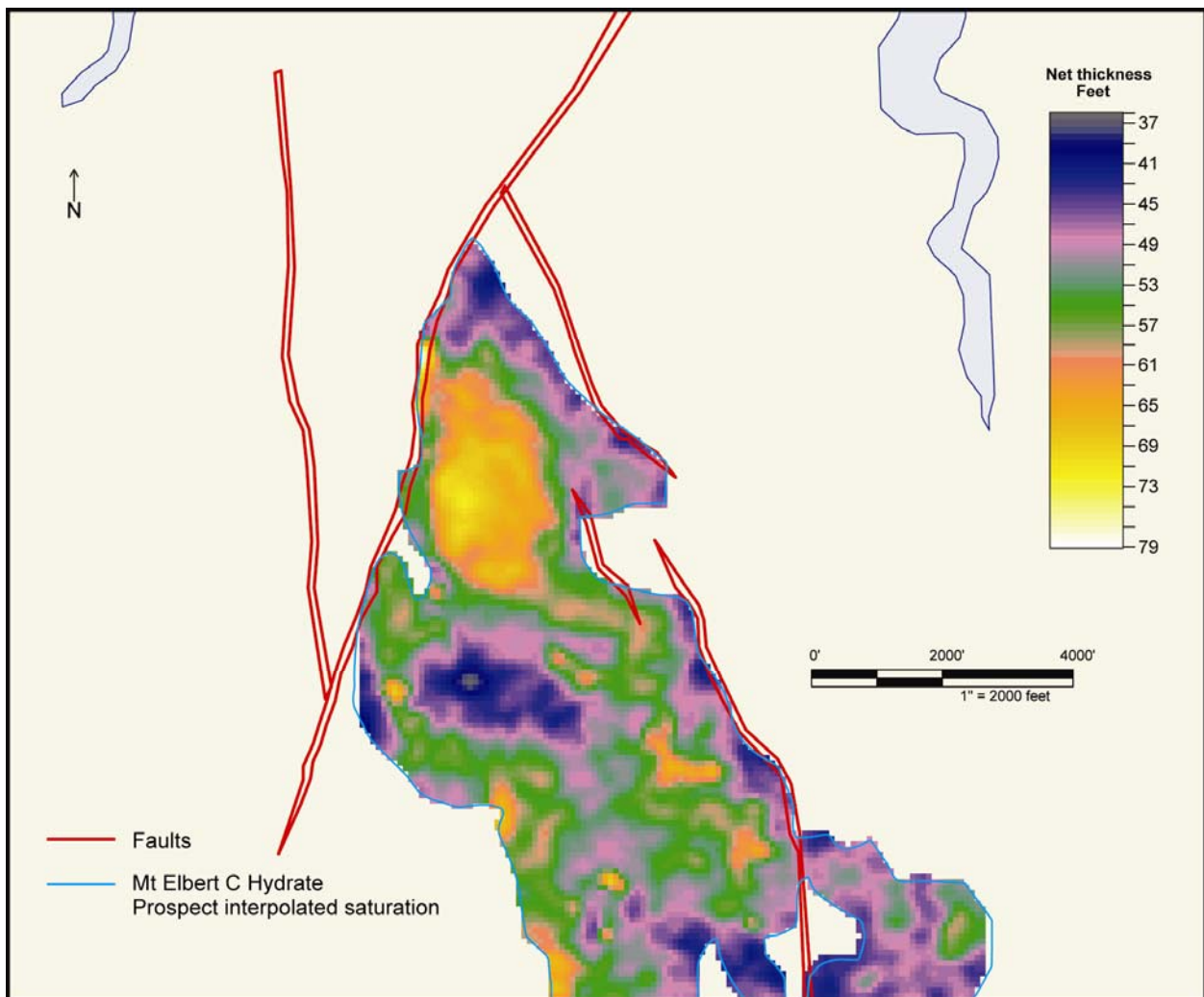


**Figure 26.** This display is a thickness map for the Mt. Elbert prospect. Thicknesses were derived using Lee's thin-bed analysis.

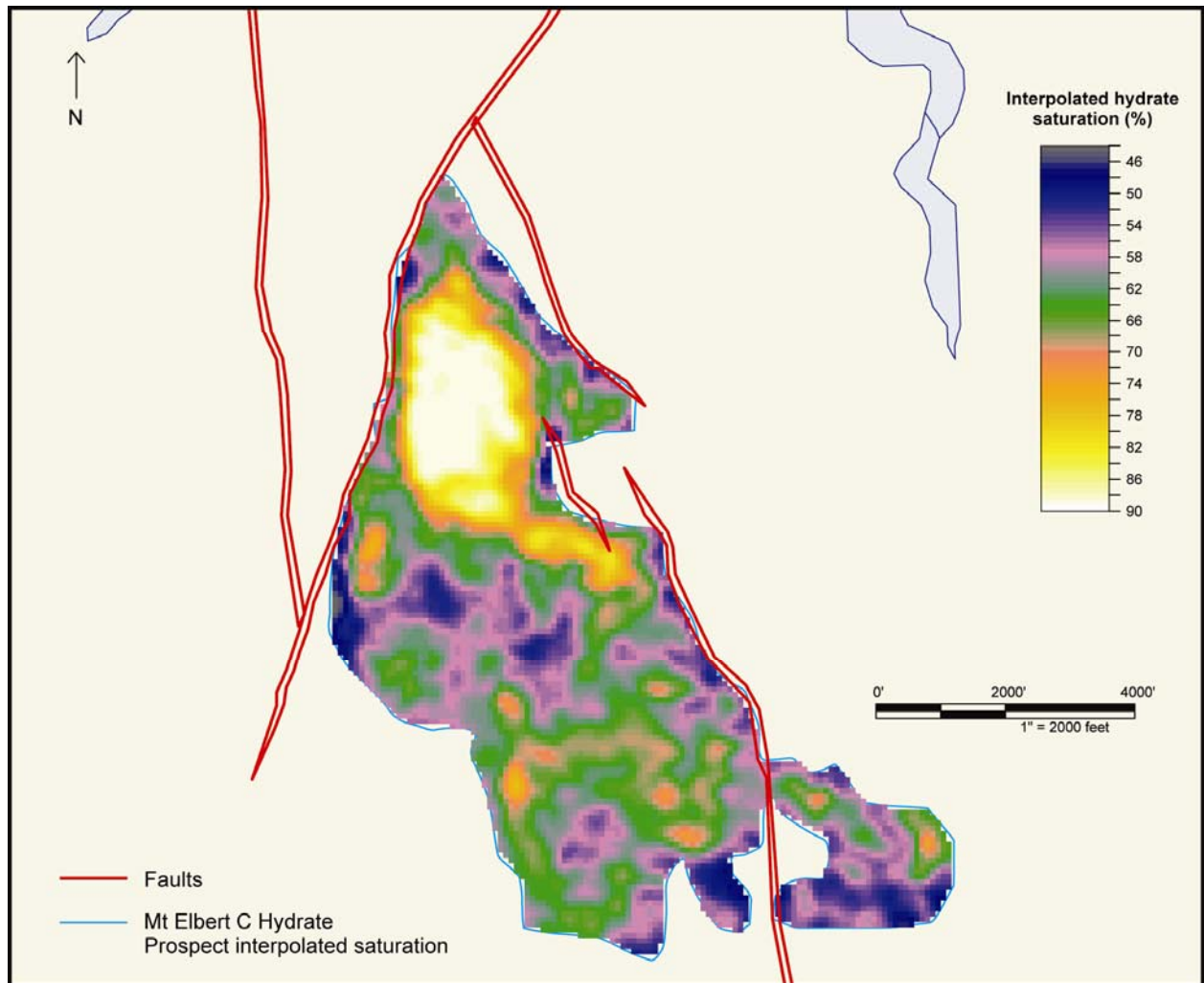


**Figure 27.** This display is a saturation map for the Mt. Elbert prospect. Saturation were derived using Lee's thin-bed analysis.

## **GAS HYDRATE VOLUMETRIC ESTIMATES**

In-place volumetrics have been computed in order to estimate the volume of gas associated with each of the gas hydrate prospects identified in this study. A number of variables, along with their appropriate distributions, minimum, most likely and maximum estimates, are required for this calculation. For this study, bulk rock volume, porosity, saturation and net to gross variables were used and applied based on specific ranges for individual gas hydrate intervals A-E (see Stratigraphic Column, **Figure 4.**)

Saturation and bulk rock volume utilized thickness and saturation calculations from seismic attributes, as in the Mt. Elbert prospect example shown in **Figures 26 and 27**. First, bulk rock volumes were calculated from grids within a robust mapping package. The computed volume was then used as the “median” value with a 10% standard deviation (1.5% standard deviations) within Monte Carlo calculations for the bulk rock volume variable using a normal distribution. Normally, calculation of net rock volume is based on the following:

1. Structural grid for the top (and / or base) of the reservoir unit,
2. Fault traces for the structural grid mapped for the top the reservoir,
3. The gas – water contact,
4. The gross interval’s isochore (vertical thickness) for the reservoir unit,
5. The net reservoir’s isochore vs the total gross isochore for the reservoir unit.

In the calculations from the “thin bed” modeling, as described for the Mt. Elbert Prospect, the model assumes gas hydrate thicknesses that are less than 1.5 times the tuning frequency. For the Milne Point 3-D survey (USGS wavelet processing) the 55 Hz. dominant frequency within the zone of interest allows us to calculate thicknesses of gas hydrate up to about 60 ft. Also, the minimum thickness is limited by frequency where gas hydrates less than 25 ft thick are acoustically transparent. Thus, the aerial limits of the gas hydrate prospects are defined by amplitude rather than faulting or structure, and the thickness calculation naturally omits areas below any down-dip gas hydrate limits. The revised list of data needed specifically for gas hydrate bulk rock volume calculation is now the following:

1. Time structure for the top of the hydrate (in this case, a trough) within the area meeting minimum amplitude criterion,
2. Time structure for the event immediately below the hydrate (a peak),
3. Amplitude difference between the trough and the peak,
4. Calculated reservoir thickness from thin-bed modeling (by trace),
5. Calculated saturation from thin-bed modeling (by trace).

From these data, calculated reservoir thickness is gridded, and summed over the area that defines the reservoir limits within the geophysical amplitude cut-offs. Bulk rock volume is reported and utilized in Monte Carlo simulations. Similarly, calculated saturation is gridded, and grid to grid calculations may be performed to estimate volumetrics as a QC to the Monte Carlo simulation results. Additionally, average saturation values from thin bed analysis were used as the median saturation value in the Monte Carlo simulations.

Regional subsurface data were analyzed to determine appropriate ranges for porosity and net-to-gross. These data varied by gas hydrate interval based on observed values in numerous wells in the Milne Point and Kuparuk River fields. **Table 3** below presents the porosity and net-to-gross values used in the volumetric calculations.

Gas Hydrate Interval	Porosity	Porosity	Porosity	Net-to-Gross	Net-to-Gross	Net-to-Gross
	Minimum	Most Likely	Maximum	Minimum	Most Likely	Maximum
"E" Gas Hydrate	37	39	40	70	80	95
"D" Gas Hydrate	36	37	38	70	80	95
"C" Gas Hydrate	34	38	40	70	80	95
"B" Gas Hydrate	34	38	40	70	80	95
"A" Gas Hydrate	34	38	40	70	80	95

**Table 3.** Parameters for volumetric calculations from subsurface control.

The distribution of saturation was determined on a prospect by prospect basis using the regional subsurface data to arrive at minimum and maximum values, 40% and 90% respectively, and using the calculated median saturation for each prospect (from seismic amplitude) as the most likely saturation for the prospect. **Table 4** below lists calculated median saturation values for each prospect in the Milne Point survey area:

Prospect Name	Median Saturation
Antero "C" Prospect	66.1
Bierstadt "D" Prospect	49.8
Bierstadt "E" Prospect	66.9
Blanca "C" Prospect	55.1
Crestone "C" Prospect	49.8
Mt. Elbert "C" Prospect	59.7
Mt Elbert "D" Prospect	52.6
Gray's Peak "B" Prospect	47.2
Maroon Peak "A" Prospect	81.2
Mt Princeton "D" Prospect	53.2
Pikes Peak "B" Prospect	68.8
Redcloud "B" Prospect	58.1
Sneffels "D" Prospect	57.6
Uncompaghre "D" Prospect	49.3

**Table 4.** Median saturations calculated from thin-bed analysis

Porosity, net-to-gross and saturation utilized a triangular distribution for the Monte Carlo simulation. In the case of the Milne Point simulation, 10,000 simulations were run. The resulting range of values resulting from the simulation model accounts for the uncertainty in every variable and provides a median value for hydrocarbon volume, and also provides an up-side (P10) and a down-side (P90.) Volumetric calculations using the Monte Carlo method were performed for each intra-hydrate prospect. The table shown in **Table 5** is an example output for

the Mt Elbert C hydrate prospect, which shows a median volume of 93.3 BCF. **Table 6** lists the calculated median in-place volumes calculated for all of the gas hydrate prospects identified within the Milne Point 3D survey. The sum of median in-place volumes for all hydrate prospects within the Milne Point area, approximately 670 BCF, is significant if they can be produced.

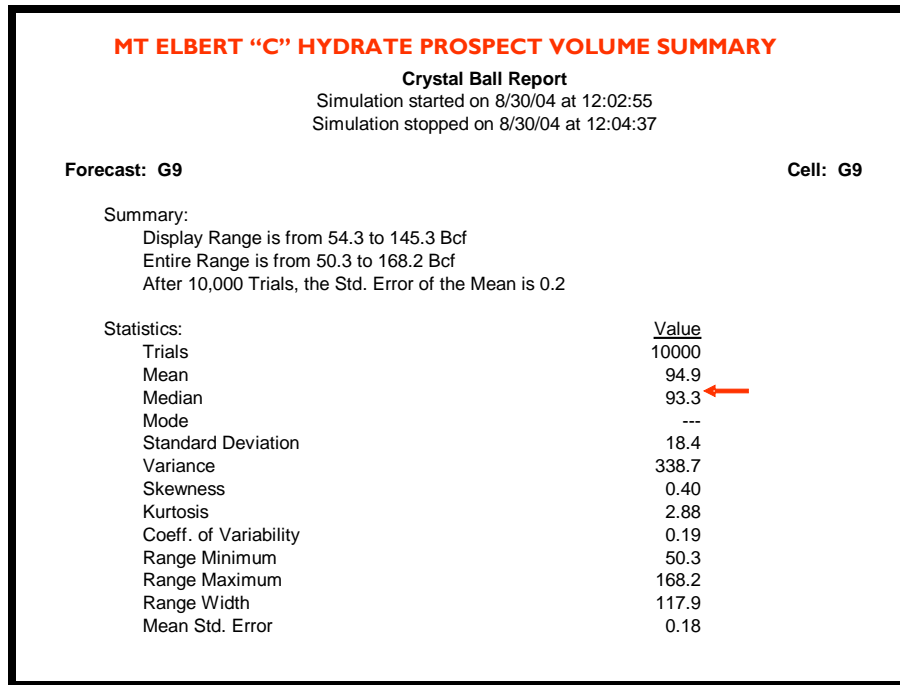


**Table 5** – Example Volumetric summary for Mt. Elbert C Hydrate prospect.

Prospect Names	Zone	closure acres	Calculated Volume BCF
<b>Hydrate Prospects</b>			
Mt. Bierstadt "E" Hydrate Prospect	E	332	41.8
Mt. Elbert "D" Hydrate Prospect	D	267	52.0
Mt. Bierstadt "D" Hydrate Prospect	D	268	32.3
Mt. Sneffels "D" Hydrate Prospect	D	516	46.2
Uncompahgre Peak "D" Hydrate Prospect	D	167	11.2
Mt. Princeton "D" Prospect	D	449	38.2
Crestone Peak "C" Hydrate Prospect	C	1728	185.8
Mt. Antero "C" Hydrate Prospect	C	955	75.2
Mt. Elbert "C" Hydrate Prospect	C	1106	93.3
Blanca Peak "C" Hydrate Prospect	C	328	22.4
Pikes Peak "B" Hydrate Prospect	B	298	13.2
Redcloud Peak "B" Hydrate Prospect	B	194	18.0
Grays Peak "B" Hydrate Prospect	B	85	5.8
Maroon Peak "A" Hydrate Prospect	A	375	32.8
<b>Total Median estimated in-place volume</b>			<b>668.2</b>

**Table 6** – Calculated Median In-Place Volumes for Milne Point gas hydrate prospects.

## **CONCLUSIONS**

The Milne Point area study has been successful in that we have been able to find both intra-gas-hydrate and sub-gas-hydrate free-gas prospects that are appropriate for the proposed production test well drilling. The historical log analysis work conducted by the USGS in this area combined with knowledge gained from 3-D seismic attribute analysis has helped us to understand the geologic setting for these unconventional reservoirs. Future drilling efforts in this area should verify assumptions used in the theoretical versus real-world modeling that were necessary to make an evaluation of the proposed prospects.

Results from structural and stratigraphic interpretation of the Milne Point 3-D survey include the following:

- 1) It is difficult to differentiate between ice and gas hydrate within the Gas Hydrate Stability Zone (HSZ) because the resistivity and acoustic properties of ice and Gas Hydrate are nearly identical. In areas where gas-hydrate and ice are commingled, the Base of the Hydrate Stability Zone (BHSZ) must be identified primarily based on the seismic response, as it cannot be directly calculated without an accurate Base of Ice Bearing Permafrost (IBPF) pick.
- 2) Within the Gas Hydrate Stability Zone, the acoustic response of water saturated, unconsolidated sandstone reservoirs, low saturation gas hydrate zones and shales are nearly the same, such that the zone has very low reflectivity. However, high amplitude zones within this interval can be attributed to higher saturation gas hydrate sections, greater than about 60% saturation, and greater than about 20 ft. thick.
- 3) On the Milne Point 3-D survey, high amplitude zones within the HSZ generally correlate to thin gas hydrates that have been identified in adjacent wells, although most of the hydrates in Milne Point wells are thinner than the minimum needed to be detected by seismic.
- 4) The unconsolidated sandstone reservoirs below the Base of the Hydrate Stability Zone (BHSZ) exhibit much higher amplitude than any events above the BHSZ even if minor amounts of free gas are present. Staines Tongue intervals in wells on the Milne Point survey exhibit low saturations of free gas below the BHSZ.
- 5) The volume of gas was calculated for each of the seismically identified gas hydrate prospects. The prospects were high graded due to the narrow seismic bandwidth that limits detection of gas hydrate bearing sections to thicknesses greater than 25 ft and saturations greater than 60%. If producible, the calculated volumes of gas in these gas hydrates may be significant as a future gas source on the North Slope,
- 6) Trace modeling shows that a significant velocity pull-up is likely to occur below zones that have high gas hydrate saturations.

Future work that may allow further insight into gas hydrate prospecting in arctic regions include the use of pre-stack migration and AVO analysis for fluid identification. This would be particularly helpful for the zone near the BHSZ, especially when accurate base permafrost depths are not available. Isochronal analysis may be important to further investigation of velocity anomalies associated with gas hydrates. This work may be important not only in understanding gas hydrates themselves, but also in correctly estimating depth for deeper targets.

## **REFERENCES**

- Bird, K.J., and Magoon, L.B., 1987, Petroleum geology of the northern part of the Arctic National Wildlife Refuge, Northeastern Alaska: U.S. Geological Survey Bulletin 1778, 324 p.
- Carman, G.J., and Hardwick, P., 1983, Geology and regional setting of the Kuparuk oil field, Alaska: Am. Assoc. Petroleum Geol. Bulletin, v. 67, no. 6, p. 1014-1031.
- Collett, T.S., 1993, Natural gas hydrates of the Prudhoe Bay and Kuparuk River Area, North Slope, Alaska: Am. Assoc. Petroleum Geol. Bulletin, v. 77, no. 5, p. 793-812.
- Collett, T.S., 2001, Natural-gas hydrates: Resource of the twenty-first century?, *in* Downey, M.W., Threet, J.C., and Morgan, W.A., eds, Petroleum provinces of the twenty-first century: Am. Assoc. Petroleum Geol. Memoir 74, p. 85-108.
- Collett, T.S., Lee, M.W., Dallimore, S.R., and Agena, W.F., 1999, Seismic– and well-log-inferred gas hydrate accumulations on Richards Island, *in* Dallimore, S.R., Uchida, T., and Collett, T.S., eds., Scientific results from JAPEX/JNOC/GSC Mallik 2L-38 gas hydrate research well, Mackenzie Delta, Northwest Territories, Canada: Geological Survey of Canada Bulletin 544, p. 357-376.
- Collett, T.S., Subsurface temperatures and geothermal gradients on the North Slope of Alaska, *in* Cold Regions Science and Technologies, 21 (1993) Elsevier Science Publishers B.V., Amsterdam, p. 275-293.
- Dillon, W.P., Lee, M.W., Fehlhaber, K., and Coleman, D.F., 1993, Gas hydrates on the Atlantic continental margin of the United States – Controls on concentration, *in* Howell, D.G., ed., The future of energy gases: U.S. Geological Survey Professional Paper 1570, p. 313-330.
- Grantz, A.M., Holmes, M.L., and Kososki, B.A., 1975, Geologic framework of the Alaskan continental terrace in the Chukchi and Beaufort Seas, *in* Yorath, C.J., Parker, E.R., and Glass, D.J., eds., Canada's continental margins and offshore petroleum exploration: Canadian Society of Petroleum Geologists Memoir 4, p. 669-700.
- Gray, W.C., 1979, Variable norm deconvolution: Stanford, California. Stanford University, Ph.D. thesis, 101 p.
- Gryc, G., 1988, Geology and exploration of the National Petroleum Reserve in Alaska, 1974 to 1982: U.S. Geological Survey Professional Paper 1399, 940 p.
- Jones, H.P., and Speers, R.G., 1976, Permo-Triassic reservoirs of Prudhoe Bay field, North Slope, Alaska, *in* J. Braunstein, ed., North American oil and gas fields: Am. Assoc. Petroleum Geol. Memoir 24, p. 23-50.

Kvenvolden, K.A., 1993, Gas hydrates as a potential energy resource – A review of their methane content, *in* Howell, D.G., ed., The Future of energy gases: U.S. Geological Survey Professional Paper 1570, p. 555-561.

Lee, M.W., Collett, T.S., and Inks, T.L., (in press), Basis of seismic attribute analysis for gas hydrate and free-gas prospects on the North Slope of Alaska; AAPG Hedberg Proceedings.

Lee, M.W., Hutchinson, D.R., Dillon, W.P., Miller, J.J., Agena, W.A., and Swift, B.A., 1993, Method of estimating the amount of in situ gas hydrates in deep marine sediments: Marine and Petroleum Geology, v. 10, p. 493-506.

Lee, M.W., 2006, Well Log Analysis to Assist the Interpretation of 3-D Seismic Data at the Milne Point, North Slope of Alaska, U.S. Geological Survey, Scientific Investigations Report 2005 5048.

Morgridge, D.L., and Smith, W.B., 1972, Geology and discovery of Prudhoe Bay field, eastern Arctic Slope, Alaska, *in* King, R.E., ed., Stratigraphic oil and gas fields-classification, exploration methods, and case histories: Am. Assoc. Petroleum Geol. Memoir 16, p. 489-501.

Seifert, W.K., Moldowan, J.M., and Jones, J.W., 1979, Application of biological marker chemistry to petroleum exploration: Tenth World Petroleum Congress, p. 425-440.

Sloan, E.D., 1997, Clathrate Hydrates of natural gases (2nd ed.): New York, Marcel Dekker Inc., 705 p.

Taylor, D.J., et al., 2003, Imaging Gas-Hydrate Bearing Zones Using 3-D Seismic Data- Milne Point, North Slope, Alaska: abstract 2003 3-D Symposium, Denver, Colorado.

Tailleur, I.L., and Weimer, P., eds., 1987, Alaskan North Slope geology: Bakersfield, California, Pacific Section, Society of Economic Paleontologists and Mineralogists and the Alaska Geological Society, Book 50, v. 1, 874 p.